Micromorphological indicators for degradation processes in archaeological bone from temperate European wetland sites

Hans Huisman*[1]

Kristin Ismail-Meyer[2]

Barbara M. Sageidet[3]

Ineke Joosten[1]

1 Cultural Heritage Agency of the Netherlands, P.O. Box 3800, 1600 BP, Amersfoort, The Netherlands, h.huisman@cultureelerfgoed.nl

2 Integrative Prehistory and Natural Sciences (IPAS), University of Basel, 4055 Basel, Switzerland, Kristin.Meyer@unibas.ch

3 University of Stavanger, Faculty of Arts and Education, N-4036 Stavanger, Norway, barbara.sageidet@uis.no

* *Corresponding author*

Abstract

Micromorphological investigations of archaeological bones make it possible to study decay processes and the associated depositional environment in one go. A selection of micromorphological thin sections from soil samples from three wetland sites in Switzerland, The Netherlands and Norway that contained bone fragments were studied. Goal was to investigate the type and the timing of decay processes to better understand the taphonomy of bones in such sites. Using optical microscopy and scanning electron microscopy with energy dispersive X-ray spectroscopy (SEM-EDX), a range of biological decay processes and chemical/mineralogical transformations were observed. In two of the sites – Zug-Riedmatt in Switzerland and Hazendonk in The Netherlands – a relatively short exposure to adverse conditions must have occurred: Some of the bones from Zug-Riedmatt show localized collagen decay related to exposure to fresh ashes; others show cyanobacterial tunnelling related to submersion in shallow, clear water. In Hazendonk, bone fragments and fish scales apparently have first been exposed to bacterial decay related to putrefaction. Subsequently, alternations between wet and dry conditions resulted in the dissolution of some of the bone mineral and the formation of Ca, Fe(III) phosphates, probably mitridatite. Fungal decay caused extensive tunnelling of bone and fish scales as well as the secondary phosphates. These processes apparently ended when the bone-rich layer became permanently waterlogged and anoxic. In Stavanger, bone mineral is transformed into mitridatite and possibly other Ca Fe(III) phosphates. Indications that the redox conditions are variable at present suggest that these processes are still active.

Keywords:

Taphonomy; bone decay; phosphates; fungi; bacteria; ash

1 Introduction

1.1 Degradation processes and the archaeological record

The archaeological record may contain a highly variable range of materials in the form of artefacts, human and animal remains, botanical material and soil features. Because these remains react differently to different environmental conditions, there are large differences in the chance of survival between different materials, and between different types of burial environments. Because of these differences, the archaeological record is intrinsically biased by the differential degradation of artefacts and ecofacts. Those remains that have a large chance of surviving ages of burial – like stone and ceramic objects – are present in most archaeological contexts. Fragile or easily degraded remains on the other hand – like the non-carbonized tissue of plants and soft animal parts – are much rarer, and moreover mostly restricted to specific environments (in essence extremely wet, dry or cold). For archaeologist, it is therefore of primary importance to take into account which types of materials can survive long-term burial in various soil environments (Renfrew and Bahn 2012 and Huisman 2009).

From experience, a general idea on the effects of the burial environment and the chance of survival of specific archaeological materials has formed. And this is generally taught in archaeological training as part of the curriculum (see e.g. Wood and Johnson 1978). In the last few decades the emergence of the "preservation *in situ*" paradigm drove more targeted research into degradation of specific materials and the role of the burial environment (see Huisman (2009) and Canti & Huisman (2015) for an overview).

1.2 Analysing and identifying bone degradation

Many bone decay processes have been identified by analysing polished bone sections with microscopes (Jans et al, 2002, 2004, Jans, 2005, Tjelldén 2016) or electron microscopes (Bell et al. 1991, Bell 2012, Tjellden et al. *in press*, Turner-Walker 2012), i.e. by histological methods. For this purpose, bone is first cut in longitudinal and/or transversal sections. Subsequently these fragments are usually (but not always; Fernández-Jalvo et al. 2010) embedded in resin, and polished. Polishing is sufficient for electron microscopy or microscopic analyses using incident light. For microscopic analyses using transmitted light, samples are usually ground to a standard thickness of c. 80 micron prior to polishing, although e.g. Jans (2005) ground the samples to 30 micron thickness which is better suited to recognize decay features

Histological analyses on bone samples has been instrumental in identifying a range of (micro) biological and chemical processes that affect forensic and archaeological bone (Bell 2012, Fernández-Jalvo et al. 2000, Hacket, 1981, Hedges et al. 1995, Hedges 2002, Hollund et al. 2012, Jans et al. 2005, Nielsen-Marsh & Hedges 2000, Smit et al. 2007, Trueman & Martil 2002, Turner-Walker 2012, Turner-Walker & Jans 2008). The method has several disadvantages, however, when applied to bones from archaeological sites: Firstly, in archaeological contexts it can only be done on bone or bone fragments that are large and firm enough to prepare oriented cross sections. This excludes small bones and bones or bone fragments that are degraded to such an extent that they cannot be isolated or mounted – or even recognized macroscopically. Secondly, bones are taken out of their context and burial environment prior to histological preparation. The direct connection between the bone and evidence for past and present burial conditions, i.e. the embedding sediment, is lost in the process. This is especially important for those cases where the present burial environment differs from that in the past – which is a common phenomenon in many archaeological sites. Thirdly: many hand-collected large bones extracted directly from the archaeological sites are air dried and washed with water, removing possible degradation features on their surfaces. Because of the correlation between burial environment and bones, histological study of bone fragments has been employed in several archaeological heritage management studies to assess present-day threats to archaeological sites (Huisman et al. 2008, Huisman 2009). On the UNESCO world heritage site of Schokland (Huisman & Mauro 2013), and during research on the middle Neolithic site of Swifterbant S4, the degree of degradation was found to vary to such a degree that it was concluded that much of the decay had taken place as a taphonomical process, i.e. before and shortly after burial.

Soil micromorphologists study polished thin sections from resin-impregnated undisturbed soil samples using microscopical techniques. Transmitted light - and polarization microscopy (PPL/XPL) can be supplemented with incident light (IL) and ultraviolet or Blue light fluorescence microscopy (UV resp. BLF), scanning electron microscopy (SEM) and a range of analytical techniques. Undisturbed soil samples are impregnated with resin, thin sections are cut from the impregnated samples, mounted on a glass plate and subsequently polished and lapped to a thickness of 25-30 microns. The combination of minerals, organic materials, their distribution and the soil structure forms evidence for present and past processes and hence for the development of soils and the burial environment (Stoops 2003, Stoops et al. 2010).

For the study of bone decay a main advantage is that smaller and strongly decayed bone fragments can still be studied, thus not only allowing decay studies in more archaeological sites but also making the study of advanced decay processes possible. The use of ultraviolet and Blue light fluorescence microscopy is especially suitable for studies on bone decay as many phosphate minerals – including bioapatite – have fluorescent properties that may be affected by heating or degradation processes (Karkanas & Goldberg 2010, Villagran et al. *in press*). But at least as important may be the potential to identify past, terminated decay processes and combining them with evidence for past, altered burial conditions (Huisman et al. 2009). A main disadvantage, however, is that the orientation of the bones and bone

fragments in a thin section is random. This makes it not only hard to recognize type of bones; it is not ideal when decay patterns are to be compared to those from histological sections.

1.3 Bone degradation

From a point of view of degradation processes, bone is one of the more complex materials that can occur in archaeological sites: It consists basically of an intricate combination of some 70% mineral material (carbonated hydroxyapatite or HAP), organic material (mostly collagen but also osteocalcine; both proteins), and 7-8% tightly bound water in a fresh bone. On a microstructural level these components are intimately connected in lamellae of several microns thick, protecting each other due to their intimate association (Collins et al. 2002, Turner-Walker 2009, Huisman et al. 2009). Several different pathways of (micro)biological, chemical and physical decay or transformation processes in bone are known. Which of these processes occur depends on the burial environment (see e.g. Collins et al. 2002 and Turner-Walker 2009). Pathway 1, following the terminology of Collins et al, (2002), entails the slow chemical degradation of collagen. Evidence for this pathway is rare, as this process is extremely slow in most burial environments. Only (pre-burial) heating and burial conditions with extreme pH are capable to speed up this process enough to have a noticeable impact on the bone structure. Pathway 2 is the chemical deterioration of the HAP. This process is restricted to neutral to acidic environments, as HAP is stable in lime-buffered burial conditions (with pH ~8.2). It is not only exacerbated by low pH, but also by fluctuating hydrological conditions and/or metal-binding humic substances that prevent the establishment of chemical equilibrium between HAP and the burial environment (Collins et al. 2002, Turner-Walker 2009). Pathway 3 consists of several types of microbial decay. With the potential exception of tunnelling by cyanobacteria (see below), initial HAP dissolution following pathway 2 is instrumental in facilitating the (much faster) processes of microbial decay (Collins et al. 2002).

Microbial bone degradation comes in several types, which were first distinguished by Hacket (1981). He identified four types of decay patterns that are related to different agents: Linear longitudinal, lamellate and budded microfocal destruction sites ("mfd's") are attributed to decay by bacteria (see also Jans et al., 2004); From the discussion in Trueman & Martil (2002) it becomes clear that it is likely that different types of bacteria are involved successively to produce these decay patterns. The bacterial decay is generally linked to putrefaction processes that can only proceed when soft body tissue is still present (Jans 2005, Fernández-Jalvo et al. 2010). The fourth type, Wedl tunnelling, is attributed to fungal decay (Hacket, 1981, Trueman & Martil, 2002, Bell et al. , 1991). Because it depends on initial dissolution of HAP, fungi can degrade bone only as long as the environment is moist (but not waterlogged), oxygenated and the pH is natural to acidic (i.e. not lime-buffered) (Huisman et al. 2009). In addition to these decay patterns, bone from underwater environments can show another type of tunnelling that is restricted to the outer surface layers of the bone. This tunnelling is most commonly attributed to decay in marine or fresh water by cyanobacteria (Bell et al. 1991, Turner-Walker 2012, Bell 2012).

The degree of microbial decay in histological samples is commonly expressed following the Oxford Histological Index (OHI; see Hedges et al., 1995) This – according to the developers somewhat subjective – index classifies the degree to which original microstructure of the bone is retained, ranging from 5 (virtually indistinguishable from fresh bone) to 0 (no original features identifiable, other than Haversian canals). Since its development by Hedges et al. (1995), this index has been used widely to quantify the degree of bone degradation. It is noteworthy that Hedges at al. (1995) apply the method to transversal cuts only, and that they implicitly seem to assume that destruction comes in the form of foci, and that haversian channels were present in the bone. Some types of degradation – especially collagen deterioration and dissolution of HAP – may result in the loss of birefringence, but are not related to include destructive foci. Jans (et al. 2002) introduced the Birefringence Index (BI) that uses the degree of birefringence to indicate collagen and/or HAP degradation. Possible index values are 1 (normal, comparable to fresh bone), 0.5 (reduced) or 0 (absent). In a recent modification of the OHI, Hollund et al. (2012) introduced the General Histological Index (GHI). It follows the same scale of 5 to 0, but also incorporates microstructure destruction by non-microbial processes and staining (see table 1).

Decay of bones in cave environments in many cases is strongly influenced by phosphate-rich deposits of bat guano. Uric and humic acids promote the dissolution of bone mineral and the formation of a range of phosphate minerals like dahlite, crandallite and montemeryite (Golberg and Nathan 1975; see Canti & Huisman 2015 for a recent literature review of diagenetic processes in archaeological cave sites). Adderly et al. (2004) investigated the origin of phosphates in medieval middens, and found nanostructural evidence that they were derived from decaying bone.

1.4 Goal of this study

Goal of the present paper is to investigate the decay patterns that may occur in bone fragments in wetland sites, and to link the decay processes with site conditions. We use micromorphological thin sections with evidence for bone degradation from various European wetland settings (Norway, Switzerland and the Netherlands). They were selected from sample series that were collected for micromorphological research projects in wetland settings, and that demonstrate a range of bone decay features. They form examples of the type of degradation processes that can be encountered in archaeological wetland sites. Degradation processes and their relation to the (reconstructed) burial environment, based on the micromorphological observations, supplemented with additional analyses on some of the impregnated samples.

1.5 The investigated sites and samples

The Neolithic lakeside settlement Zug-Riedmatt (Canton Zug, Switzerland) was discovered in 2006 due to geological subsoil investigations at the northern rim of lake Zug. The dating is about 3200 to 3100 cal. BC based on ceramic typology (Horgen period; Huber & Schaeren, 2009). The > 1 m thick cultural layer is situated on top of limnic calcium carbonate sediments consisting mainly of micrite ("lake marl"), at the interface with the former river Lorze delta, and is covered by more than 6 m of deposits of limnic and deltaic fluvial origin. 64 m^2 of the site was excavated in 2008 by the Department of Monument Conservation and Archaeology of the Canton Zug, and sampled densely for interdisciplinary research (130 profile columns of up to 25-56 cm height). From 2014 to 2016, the site was part of a research project concerning formation processes and taphomomy of wetland deposits with the aim to obtain detailed information about the complex interplay between layer formation, preservation and degradation processes in the amphibious context of lakeshore wetland deposits (see e.g. Steiner et al., 2017; Ismail-Meyer et al., *in prep*.). Since 2011, the site belongs to the UNESCO World Cultural Heritage "Prehistoric Pile dwelling around the Alps".

For the present study, we concentrate on a bone midden: It consists of an accumulation of about 3200 large bone fragments (mainly red deer; at least 36 individuals), more than 3000 small bones (frog and fish remains), collected and harvested plants (i.e. poppy, flax seeds, cereal bran), artefacts, carbonate wood ashes, loam and sand (see also Billerbeck et al. 2014; Billerbeck-Braschler, 2016). The major part of the large animal bones was probably deposited in a single event in late spring/early summer during an early settlement phase . Since there is evidence that about 15% of the bones have been transported somewhat in the direction of the lake and parallel to the shore – leaving no trace of macroscopic abrasion – this probably occurred during a phase of higher lake water table. On top of the bone midden, fish and amphibian bones (grass frog, pike, perch, carp and whitefish) form a dense layer together with calcitic ashes, indicating a deposition of the layer from spring to late autumn and winter (Figure 1) (Billerbeck et al., 2014; Billerbeck-Braschler, 2016). In this paper, we present observations from profile columns ZGRI 84A, B and 98A, which form a stratigraphic sequence through the bone midden (Figure 1).

Hazendonk is a Pleistocene riverdune, in the Holocene floodplain of the Rhine-Meuse delta in the West of the Netherlands. An extensive excavation in the 1970'ies on the flanks of this dune revealed a series of refuse layers from Middle to Late Neolithic age (c. 5000-2900 cal. BC), intercalated with peat and fluvial clay. Due to the well-separated stratigraphic levels, Hazendonk is a key site in the typochronology of the Dutch Neolithic; the Hazendonk culture is named after this sites (Louwe Kooijmans 2005). The well-preserved remains from the site play an important role in the discussion on the neolithization process and paleoecological development in the Dutch wetlands (e.g. Out (2010), Amkreutz (2013) for recent examples).

Soil scientists from Wageningen University took a series of samples for micromorphological research during the 1976 campaign. In Exaltus & Miedema (1994), a summarily characterization of these samples is given. The thin sections are stored at the International Soil

Reference and Information Centre (ISRIC) in Wageningen. The impregnated samples ("blocks") from which the thin sections were made have been discarded at an unknown date.

Bone decay features were observed in one of the thin sections (no. 77110) when the Hazendonk thin sections were on loan to the Cultural Heritage Agency in Amersfoort for comparison with other wetlands sites. This sample originated from the deepest peat layer, which is dated to c. 4000 cal. BC (Figure 2).

The Stavanger site is located in the city centre. The city lies on Quaternary glacial (mostly till) deposits on the lower Jæren coastal plain (Raunholm et al. 2003) that cover Precambrian granodioritic and mica gneisses (Jorde et al. 1995). These deposits were flooded – the Late Glacial Marine Limit (ML) was about 25 m above present sea level around Stavanger (Andersen et al. 1987). The site formed on top of these deposits and is essentially characterized by anthropogenic processes of accumulation and transformation.

The Norwegian Institute for Cultural Heritage Research (NIKU) has carried out archaeological excavations in the city centre. They were executed 2004-2006 on behalf of Stavanger municipality, and in connection with restoration and a new construction of the historic market place. Archaeologists investigated several localities between the bay and quay, and the c. 1100 AD cathedral.

Independent of the NIKU project, permission was given to take 13 soil samples for micromorphological analysis (Sageidet *in prep.*). These samples were taken between 80-260 cm depth (above the groundwater table), from a North-facing profile, about 60 m from the cathedral – 150 m from the present quay – and 70-80 m from the AD 1100 shoreline (Sandvik *in prep.*). The observations in the present study were done on thin section nr. 5 (Figure 3), sampled from 237-249 cm below surface and about 10 cm below a layer dated to ca. AD 900-1100 (Sandvik *in prep.*).

2 Materials and methods

2.1 Samples and sample processing

An overview of site characteristics and analysed samples is given in Table 2. Samples from the three sites were processed by the same general preparation method for micromorphological thin sections (e.g. Beckmann, 1997): First the water in the soil samples was removed by drying (Zug and Stavanger) or by replacing it with acetone (Hazendonk). The latter method is time-consuming, but especially useful for preserving organic tissue and easily oxidized minerals. Next, the samples were impregnated with slow-hardening epoxy or polyester resin under vacuum, producing hard, undisturbed soil samples. The three 10 x 24 cm Zug samples were cut in several sections, from which a total of 11 subsamples were taken for thin section production (see e.g. Ismail-Meyer et al., 2013). One thin section was made from each of the two complete Hazendonk and the Stavanger samples.

Thin sections were made by first polishing one side of the sample and gluing it to a glass plate. Subsequently, it was cut, polished and lapped to a standard thickness of 25 – 30 micron and covered with a glass cover slip (e.g. Beckmann, 1997). The impregnated soil sample ("block") of the Hazendonk sample has gotten lost some time after thin section preparation in 1976, but the blocks from Zug and Stavanger were still available for further research.

From the thin sections that contained bone samples, a selection was made that encompassed the range of taphonmical processes present in the sample series.

2.2 Methods

The thin sections were studied in the labs of the Cultural Heritage Agency, IPAS and at the University of Stavanger using an Axioskop 40 polarization microscope with fluorescence option (magnification 25-1000 x), a Leica DMRXP polarization microscope (magnification 16 – 630 x), a Leica Laborlux fluorescence microscope (magnification 50-400 x) and an Olympus BX51 (magnification 40-400 x). The impregnated soil samples ("blocks") from Stavanger and Zug-Riedmatt were also studied under low magnifications with incident light using a Leitz/Wild M420 with a magnification of 6.5-35x. Further, they were polished by hand and studied using a JEOL JSM5910LV Scanning Electron Microscope (SEM, 20 kV, 30 Pa) at the Amsterdam lab of the Cultural Heritage Agency. The samples were not coated. Chemical surface analyses on the samples were done by energy dispersive X-ray spectroscopy (EDX, SDD detector from Thermo Fisher Scientific and NSS software), using spot measurements and element mappings (detection limits c. 0.1 %). P-analyses were recalculated to PO_4 to easy stoichiometric calculations in the tables and graphics. XRD analyses in the same lab did not yield useable results.

3 Results

3.1 Morphological observations:

Zug-Riedmatt

The Zug-Riedmatt profile samples ZGRI 84 and 98 show at the base the undisturbed limnic carbonate rich sediments, followed by a thin organic transition layer to the bone midden sediments, containing large amounts of bones/antler, organic matter, loam aggregates, ashes, charcoals and sand (Figure 1). The midden shows alternations between layers rich in micritic calcium-carbonate aggregates that are interpreted as remains of calcitic wood ash, and layers rich in phosphate-impregnated ashes and silica slag (melted phytoliths) but lacking in calcitic wood ashes. Layers rich in loam and fish bones characterize the upper part of the bone midden. Loam fragments originate probably from human activities or raw material processing in the dwellings of the lakeshore settlement.

The thin sections are extremely rich in partly burned bone fragments of red deer, amphibians and fish. The bones in general are well preserved and almost unaltered, with a GHI class 4-5 (after Hedges et al. 1995). Surface tunnelling on some bones is the only biological evidence for bone decay (Figure 4A-C), observed mainly in the lower and intermediate layers of the midden. Some signs of bone dissolution (widened pores), orange iron precipitation in pores, and surface flaking can be recognized in the shallowest part of the bone midden, and some fragments show darkening and (shrinkage) cracks in the near-surface area of bones (Figure 4 D-G). With crossed polarizers (XPL) and fluorescent light (UV), the cracked and darkened bone mass shows no birefringence and fluorescence, whereas the unaltered bone is birefringent and fluorescent (Figure 4H-J). Some fish scales embedded into calcitic ashes show also darkening and a kind of micro-aggregation at their surface (Figure 4K and L). Other bones show in some cases darkening combined with surface tunnelling (Figure 4M and N).

Hazendonk

In the lower part of Hazendonk slide 77110 two composite layers, intercalated between peat and sand deposits (Figure 2A-C), were described by Exaltus & Miedema (1994) as “a thin layer consisting almost entirely of bone” and later in the paper as a layer of fish scales. Indeed, the uppermost part of this layer consists mostly of bone, most of them recognizable as fish scales by their elongated shape and saw-tooth edge. The bone fragments and fish scales have a yellow to slightly orange colour in plane polarized light (PPL). Many of the scales at the top of the deposit show signs of intense Wedl-type tunnelling (Figure 5A). Some of the scales instead show complete budded type mfd’s that left a pattern of minute tunnels while preserving only the outer rim (Figure 5B). The bones in this layer therefore fall in GHI class 0-1.

The rest of the layer consists of a groundmass that can be described as layered, yellow- to orange-brown massive homogeneous material, which is not birefringent in crossed polarized light (XPL). This material incorporates various small objects – like a fragment of burnt bone

and charred plant remains. It contains (birefringent) bone fragments that have irregular and sometimes (seemingly) gradual transitions to the surrounding material (Figure 5C- E). The massive material is fluorescent under Blue light (BLF) (Figure5F), but not under UV light (Figure 5G). The material gives the impression of having been plastically deformed, e.g. where a fragment of burnt bone has been pressed into it (Figure 5H, I). Its groundmass seems to be massive, but in many places on closer inspection it appears to be riddled with small Wedl-like tunnels, which are best visible in incident light (Figure 5E, H, I).

Stavanger

The sample from Stavanger consists mostly of coarse minerogenic sediments and rock fragments, and contains some organic materials like charcoal and bones. It does contain a domain that is a few cm across; upon closer inspection it consists of angular accommodating fragments of bone (Figure 6A). These fragments are associated with or embedded in a yellowish-orange massive material, similar to the material described above in Hazendonk. In some areas this material shows fan-shaped or irregular patterning (Figure 6D). Both this material and the bone fragments are only locally birefringent (Figure 6B, E). The remaining bone fragments are fluorescent in Blue light (BLF); hence, the massive surrounding material sometimes is (Figure 6F), and sometimes is not (Figure 6C). These bone fragments would fall in GHI class 0. Secondary manganese (hydr)oxides are recognizable as black spots near the original surface of the bone.

3.2 SEM-EDX analyses

SEM images of the Zug-Riedmatt block show in general well-preserved bone with hardly any evidence for alteration. The few zones where bone was altered could be identified in the SEM-images of the polished blocks by their pattern of fissures (Figure 7A). EDX spot analysis on such altered and unaltered bone give spectra that are dominated by calcium (Ca) and phosphorous (P) and only traces of other elements (Figure 7B and C; Table 3). Carbon and oxygen (C, O) should be disregarded in these spectra, as they may be influenced by the impregnating resin used to make the blocks.

Since the polished blocks from Hazendonk are not available anymore, no SEM analyses were possible on these samples.

The bone fragments in the SEM-images of the Stavanger polished block appear massive, whereas the massive-like material apparently consist of rounded grains – a few micron across at the most – with slightly stronger attenuation (lighter colours; see Figure 8A). EDX spot analyses show more iron (Fe) in the unaltered bone than in those from Zug-Riedmatt. The massive material has lower Ca and higher Fe (Figure 8B,C). SEM-EDX mappings (Figure 8 D - G) corroborate that the massive material has lower Ca and high Fe concentrations.

4 Discussion

4.1 Identification of decay processes

Table 4 contains a summary of the observed bone decay features. Several of these features can be linked to known processes:

Budded mfd's – like the ones in some of the Hazendonk fish scales (Figure 5B) – are usually linked to bacterial decay during putrefaction (Trueman & Martill 2002, Jans 2005, Fernández-Jalvo et al. 2010). Through and through Wedl tunnelling however, also seen in Hazendonk (Figure 5A), are attributed to fungal decay (Hacket, 1981, Trueman & Martil, 2002, Bell et al., 1991). The surface near tunnels in some of the Zug-Riedmatt bones are not Wedl-tunnes (Figure 4A-C, 4M and N); the size and character indicate that they were made by cyanobacteria (Turner-Walker & Jans 2008, Turner-Walker 2012) while submerged in lake water.

The discolouration, shrinkage and cracking patterns observed in some parts of the Zug-Riedmatt bones has been linked with (quick) collagen loss due to chemical degradation, described e.g. by Jans (2005) (Figures 4D-N): The pattern of the aggregated surface of some fish bones seems to indicate some sort of (biological?) reprecipitation process; the strong fluorescence of the material suggests that we are dealing with apatite or dahlite (cf. Goldberg & Nathan 1975). Lacking comparable observations we cannot determine so far what kind of process is responsible for this (Figure 4 K and L).

The optical properties of the yellowish massive material in the samples from Stavanger and Hazendonk are very similar. Without the impregnated blocks from Hazendonk it is not certain but we are most likely looking at the same material in Hazendonk and Stavanger. Yellowish-orange phosphatic material has until now not been found in association with decaying bone (cf. Villagran et al. *in press*). However, the material seems similar to that of calcium-iron phosphates that are a common feature in soil thin sections from archaeological settlement sites (e.g. Simpson et al. 2000, Adderley 2004). In the sites under investigation here, however, the phosphates occur only in or associated with bone fragment(s). This is a strong indication that the formation of this material in these sites is a result of processes that are related to a form of bone decay, and not a precipitate associated with the overall burial environment.

The SEM-EDX spot-analyses on the Zug-Riedmatt and Stavanger samples (Table 3 and Figure 9A) give clues about the changes in bone composition during chemical decay and the composition of the massive material. Compared to the unaltered bone, the altered bone in the Zug-Riedmatt sample shows slightly lower concentration of Ca and PO_4. The Ca/PO_4 ratio lies close to hydroxyl apatite and bone mineral. The lower mineral concentrations are remarkable: The decay pattern observed microscopically is usually interpreted as resulting from the decay of collagen only. The mineral concentration should then remain the same –

maybe even increase because shrinkage would concentrate the remaining material more (Turner-Walker 2009). It is therefore most likely that some of the bone mineral was also lost in this decay process.

In the Stavanger samples, all bone fragments have lower Ca and PO_4 contents than the Zug-Riedmatt bones. Moreover, the Ca/PO_4 ratio is lower than expected, even in the seemingly unaltered bone fragments. The analyses on the massive material form a cluster with even lower Ca values and Ca/PO_4 ratios (Figure 9A). The lower values are compensated with iron: Figure 9B demonstrates that all Stavanger samples have much higher Fe concentrations and Fe/PO_4 ratios that compensates for the lower Ca/PO_4 ratios.

On the basis of these analyses, the massive material can be identified as a Ca-Fe phosphate. Its composition lies close to that of mitridatite ($Ca_6(H_2O)_6Fe(III)_9O_6(PO_4)_9 \cdot 3H_2O$ (after Roberts and Brown 1979; www.mindat.org) – simplified as $Ca_2(H_2O)_2Fe(III)_3O_2(PO_4)_3 \cdot H_2O$ – although Nriagu & Dell (1974) and Stamatakis & Koukouzas (2011) give it as $CaFe_2(PO_4)_2(OH)_2 \cdot 8H_2O$). The seemingly unaltered bone from Stavanger appears to form a mix of mitridatite and bone mineral (approached by ideal Hydroxylapatite), but we cannot exclude that other minerals are involved as well.

Mitridatite is a mineral that is known to be associated with bone decay processes: Roberts and Brown (1979) suggest that mitridatite in Ethiopian lacustrine sediments precipitated together with prismatic hydroxyapatite crystals following (partial) dissolution of fish scales and bones. They describe the mineral as greenish brown to yellowish green, with small (2-2.5 micron) composite, saddle shaped and feathery crystals. This colour description – and that of Karkanas and Goldberg (2010), who give mitridatite colour in thin sections as red, green or brownish with second- or higher order colours with crossed polarizers (XPL) – does not agree with our observations. This may be because the material in our thin sections is semi-crystalline: no phosphate minerals were detected by XRD.

Nriagu & Dell (1974; Fig. 6) describe a formation process whereby mitridatite is formed in absence of calcium carbonate by either of two processes: One pathway involves the transformation of ferromanganese oxides with added Ca^{2+} and phosphates. Another pathway is by oxidation of a combination of vivianite (Fe(II) phosphate), reddingite (Mn(II) phosphate) and/or anapaite (Ca, Fe(II) phosphate). Since our phosphates are associated with decaying bone, the second pathway is the most likely in our case. Nriagu & Dell (1974) indicate that vivianite, reddingite and anapaite may originate from various processes, including the mixing of decaying bone-derived Ca^{2+} and phosphates with Mn^{2+} and Fe^{2+} that are released in an anaerobic environment. It is remarkable that under these conditions no vivianite was formed.

The fungal-like tunnelling pattern in these secondary phosphates is remarkable: this type of tunnelling is usually only seen in bone, and attributed to saprophagic fungi. In nutrient-starved environments, however, ectomycorrhizal fungi are known to colonize and tunnel through mineral grains (Jongmans et al. 1997). Not only feldspars, but also mineral apatite has been shown to be a preferred target for these fungi (Wallander 2000, Blum et al. 2002, Hoffland et

al. 2003). It is not possible, however, to reconstruct now whether the fungi that tunnelled the secondary phosphates (and bone fragments) were saprophages of ectomycorrhizal fungi.

4.2 Implications for the burial environment

4.21: Microbial decay patterns

The microbial decay patterns observed are restricted to specific conditions: Tunnelling by cyanobacteria is restricted to underwater environments with ample sunlight, usually quite shallow (Turner-Walker & Jans 2008, Turner-Walker 2012). For the Zug-Riedmatt bones, that means that this decay process is related to phases when the bones were lying on the lake bottom near the shore, prior to their burial under sediments. The bacterial decay observed in some of the fish scales in Hazendonk is associated with putrefaction of the weak body parts – especially intestines. These processes tend to terminate when the weaker body parts have decayed (Jans 2005). Fungal tunnelling is a common feature in exposed (i.e. non-buried) bones and in bones in non-calcareous non-waterlogged environments. Since saprophagic and ectomycorrhizal fungi are both only active in aerobic environments, fungal tunnelling must have stopped when the environment became fully waterlogged.

4.2.2 Loss of collagen and the role of ashes

Loss of collagen while the mineral phase is preserved – which seems to have occurred in small areas in the bones from Zug-Riedmatt – is commonly restricted to neutral to acidic burial environments. However, it has also been linked to with extreme pH values in general as well as prolonged boiling, or the passage through a stomach (Collins et al., 2002). Thick deposits of lake marl in lake Zug, however, indicate that the lake water and burial environment must be in part lime-buffered and therefore alkaline: In the bone midden sediment, a mean pH_{CaCl2} 6.9 was measured (E. Eckmeier, pers. comm.) – roughly equivalent to 7.9 pH_{H2O} (after Boesten et al., 2015) – which would not be inductive to collagen dissolution.

The identification of carbonate wood ashes in thin sections from some parts of the bone midden, however, form an important clue: Fresh wood ash typically consists mainly of a mixture of (hydr)oxides of potassium and calcium (K_2O/KOH, CaO/$Ca(OH)_2$; e.g. Cílová & Woitsch, 2012). When submerged, or when buried under wet conditions, the K_2O readily dissolves and is transported or leached. Depending on the environment, CaO can be transformed into calcium hydroxide $Ca(OH)_2$ and subsequently into carbonates ($CaCO_3$). The tendency of calcitic ashes to dissolve and reprecipitate in larger, more stable crystals has been described by several researchers (e.g. Canti, 2003; Shahack-Gross & Ayalon 2013). The recognizable calcitic wood ashes in Zug-Riedmatt have undergone the transformation into calcium carbonate. Dissolved phosphate coming from bones and/or dung can easily

reprecipitate in calcitic ashes, making them less soluble under low pH conditions (Polo-Diaz, 2016). Under low pH conditions, calcium carbonate dissolves (Canti, 2003). This implicates that in Zug-Riedmatt, most settlement layers were originally rich in ashes; in layers with phosphatized ash and silica slag, calcitic ashes have been dissolved (see also Ismail-Meyer et al., *in prep*.). Dissolution processes may be promoted by organic accumulation in anaerobic environments: Such deposits tend to acidity due to organic matter decay, as seen in natural peats and also in the wetland site Zurich-Opéra (Collins, 2002; Pümpin et al. 2015; Blume et al. 2016).

Due to the high contents of K and Ca (hydr)oxides, fresh wood ash is strongly alkaline. Collins et al. (2002) indicate that "the funerary practice of adding lime (CaO) or slaked lime (CaOH) to corpses would have the effect of elevating pH and potentially accelerating collagen loss". If so, the same will be true for fresh wood ash.

For the site of Zug-Riedmatt, it is likely that the observed evidence for collagen loss in furthermore well-preserved bones is related to phases of calcitic wood ash accumulation under non-flooded conditions, perhaps enhanced by previous burning of some bones. Rising pH induced hydrolysis of the collagen in the embedded bones, which subsequently was leached. Figure 4M-N shows a bone fragment that has been strongly affected by collagen degradation, up to the point that it has become fragmented – although the fragments are still articulated. Cyanobacterial attack is restricted to the light-exposed part of the original bone surface. This is an indication that this decay preceded the ash-induced collagen degradation. Apparently, this bone was dumped and became submerged first, allowing cyanobacterial degradation. Subsequently, a drier phase occurred, during which the bone got mixed with or incorporated in ashy deposits. The shrinkage cracks observed in some bones are probably at least partly an artefact due to the air-drying before impregnation of the blocks (see above; *The samples*), but also an indication that the decayed bone has dried out as a part of the overall degradation process.

4.2.3 Secondary phosphates

The mitridatite (and maybe other Ca, Fe(III) phosphates) identified in Stavanger and Hazendonk form also under restricted conditions: The association with decayed bone and its absence in the surrounding soil mass indicates that the mineral is formed as part of or associated with bone decay processes. Since bone is low in iron, it had to be introduced into the decaying bone from the surrounding soil or water. However, iron ions are not mobile in most oxygenated soil environments (i.e. as Fe^{3+}), except at pH <3 (Appelo & Postma 1993). Since such low pH values are not common in the environments that we studied, transport of iron into the area of bone decay therefore must have taken place under waterlogged and reducing conditions, where iron occurs as Fe^{2+}(aq).

Following Nriagu & Dell (1974), it is therefore most likely that the bone decay and associated precipitation of mitridatite or other Ca, Fe(III) phosphates is related to alternating oxic and reducing conditions. This also ties in with the presence of manganese oxides in the Stavanger bone. Under wet, reducing conditions without lime buffering, bone mineral dissolves. The resulting Ca^{2+} and phosphates precipitate together with Fe^{2+} to form e.g. anapaite or similar phases – maybe also reddingite if Mn^{2+} is available. Durning dry periods, oxygen becomes available, forming an environment in which anapaite is unstable; the latter is transformed to mitriadite according to the following net reaction:

$$9Ca_2Fe(II)(PO_4)_2 \cdot 4H_2O + 3O_2 + 5\ H_2O + 3e^- >$$

$$Ca_6(H_2O)_6Fe(III)_9O_6(PO_4)_9 \cdot 3H_2O + 12\ Ca^{2+} + 9\ PO_4^{3-}$$

From this equation it becomes clear that this transformation results in a considerable loss of Ca and phosphates. The secondary hydroxyapatite associated with mitridatite surrounding decaying fish scales and bones observed by Roberts and Brown (1979) indicate that these Ca and phosphate ions may precipitate as hydroxyapatite – provided the burial conditions would allow it. Since authigenic hydroxyapatite was not observed in our Stavanger and Hazendonk samples, the geochemical environment apparently was not conducive (too acidic?) to its formation.

Alternating wet and dry conditions also help explain the fragmented nature of the decayed bone remains in Stavanger. It is likely that the chemically decayed bone mass shrunk during every dry spell. The precipitation of secondary phosphates kept the resulting fragments articulated.

The secondary phosphates encountered in the Stavanger and Hazendonk wetland sites differ from previously reported phosphate minerals that are related to archaeological bone decay in cave sites (Goldberg and Nathan 1975, Karkanas et al. 2000, 2002, Shahack-Gross et al. 2004). In these caves, minerals like dahlite (Ca phosphate), crandallite (Ca, Al phosphate) and montgomeryite (Ca, Mg, Al phosphate) form due to reactions with calcite or other rocks. The major difference with Stavanger and Hazendonk, however, is that these sites had (or still have) fluctuating redox conditions. In such environments, Fe^{2+} becomes available during reducing episodes, and can become oxidized to Fe^{3+} when the environment is oxidizing again. This mechanism is needed to provide enough iron and in the right oxidation state to form iron-rich Ca, Fe phosphates instead of Fe(II) phosphates like vivianite. Also calcite-buffered deposits of mature sediments like the ones at Hazendonk are unlikely to provide Al and Mg in large enough quantities to allow the formation of Mg, Al phosphates.*4.3.4. Interaction and order of decay processes*

Combining evidence for microbial decay and for chemical and mineralogical transformation make it possible to propose a sequence of decay processes that affected the bones in the three sites investigated:

In **Zug-Riedmatt**, the cyanobacterial tunnelling in the red deer bones/antlers show that the bones have been waterlogged (during and) after deposition in a phase of high water table. The

loss of collagen can be related to the deposition of calcitic (and silica) ashes with fish scales and gills after a dropping of the lake level. Since the red deer bones were accumulated during late spring/early summer and the fish and frog remains (and ashes) during early spring to late autumn and winter (see above), the accumulation and degradation patterns may have formed within a single year, reflecting also the usual migration of the lake water table from high during spring to low during summer (Keddy, 2010).

In **Hazendonk**, the bones and fish scales at first were probably deposited together with weak body parts, which resulted in intense bacterial decay in some of the scales. Subsequently, repeated alternations between reducing (waterlogged) and oxic (dry) conditions in a neutral to acidic environment drove the transformation of parts of the bones into massive Ca, Fe(III) phosphates – probably mitridatite. Charcoal fragments in the deposits below and above the layer consisting of bone and secondary phosphates, and deformations in this layer (attributed to trampling) suggest that this process was contemporary with human presence at the site. During at least some of the oxic periods – probably the latest – the material became dry enough to allow fungi to tunnel extensively through scales and secondary phosphates. Rising water tables and the deposition of new sediment layers subsequently resulted in permanently waterlogged, reducing conditions. Iron and/or manganese oxides that may have precipitated along with the secondary phosphates must have disappeared permanently when reducing conditions remained permanent.

In **Stavanger**, the strong degradation of the bone by chemical and mineralogical transformations makes it impossible to still recognize traces of microbial decay. The decay process in Stavanger is also driven by alternations between oxic (dry) and reducing (waterlogged) conditions in a neutral to acidic environment, transforming bone mineral into mitridatite. The presence of (black) manganese hydroxide staining indicates that here, contrary to Hazendonk, oxic conditions still prevail at least temporarily. It is therefore likely that bone degradation has been active until the moment of sampling.

4.2.5. Implications

It is remarkable that so many different types of bone degradation may be found in such thin layers, especially when they must have been active sequentially: In Zug-Riedmatt, we can discern within a few centimetres processes related to (1) deposition, (2) submersion, (3) drier periods and (4) burial within a waterlogged environment. In Hazendonk we see within 2 cm (1) deposition, (2) putrefaction, (3) alternating wet and dry periods and (4) burial. On the one hand, this study may serve as example how site-formation and taphonomical processes may be derived in great detail. On the other hand it may serve as warning that multiple observations may be necessary to obtain a complete picture of processes that were active around deposition.

In addition, it is important to notice that the optical properties of the secondary Ca, Fe(III) phosphates bear close resemblance to the groundmass of carnivore coprolites (see Brönniman et al., *in press*) – which are also known to contain bone fragments (Huisman et al. 2014). This

similarity may be due to the simple fact that both carnivore coprolites and the massive material we encountered mostly consist of very fine phosphate minerals. The main difference with the bone decay-related material is that phosphate-rich coprolites usually have an aggregate-dominated crumb-like groundmass. The bone decay-related phosphates on the other hand have a massive, sometimes layered groundmass or fan-shaped precipitates like in the Stavanger sample.

6 Conclusions

Our investigations on bone fragments in thin sections and impregnated soil samples from three wetland sites show evidence for a range of biological decay processes and chemical/mineralogical transformations. In two sites (Zug-Riedmatt and Hazendonk), a relatively quick burial by waterlogged sediments was instrumental in overall good preservation of bones. Still, the relatively short exposure to adverse condition has left their marks. Some of the bones from Zug-Riedmatt show first a cyanobacterial tunnelling related to submersion in shallow, clear water, and second, localized collagen decay related to ash deposits in subaereal exposure. In Hazendonk, bone fragments and fish scales apparently have first been exposed to bacterial decay related to putrefaction. Subsequently, alternations between wet and dry conditions resulted in the dissolution of some of the bone mineral and the formation of Ca, Fe(III) phosphates, probably mitridatite. Fungal decay caused extensive tunnelling of bone and fish scales as well as the secondary phosphates. These processes ended when the bone-rich layer was buried and became permanently waterlogged. In Stavanger, however, transformation of bone mineral into mitridatite and possibly other Ca Fe(III) phosphates in deposits with changing redox conditions has probably continued until the sample was taken.

7 Acknowledgements

The study of Zug-Riedmatt was supported by the Department of Monument Conservation and Archaeology of the Canton Zug and the Swiss National Fundation SNF (Project Number CR30I2_149679/1).

KIM would like to thank Gordon Turner-Walker, Sandra Billerbeck-Braschler, Eileen Eckmeier, Eda Gross, Gishan Schaeren, Stefanie Jacomet, Thomas Beckmann and Philippe Rentzel.

BS would like to thank Georges Stoops, Richard Macphail and Yannick Devos, for their help on interpretation of the Stavanger thin sections.

HH would like to thank Ad van Oostrum and Stephan Mantèl for recovering and allowing access to the Hazendonk thin sections, and Miranda Jans for helpful comments on the interpretation of some of the decay processes. Mario van IJzendoorn polished the impregnated block prior to SEM-EDX analyses.

Literature

Adderley, W.P., Alberts, I.L., Simpson, I. & Wess, T.J., 2004: Calcium–iron–phosphate features in archaeological sediments: characterization through microfocus synchrotron X-ray scattering analyses, Journal of Archaeological Science 31: 1215–1224

Amkreutz, L.W.S.W., 2013: Persistent traditions. A long-term perspective on communities in the process of Neolithization in the Lower Rhine Area (5500 – 2500 cal. BC), Sidestone press, Leiden, 545 pp.

Andersen, B.G., Wangen, O.P. & Østmo, S., 1987: Quaternary geology of Jæren and adjacent areas, southwestern Norway. Norges Geologiske Undersøkelse Bulletin 411: 1-56.

Appelo, C. A. J. & Postma, D., 1993: Geochemistry, groundwater and pollution, Rotterdam, Balkema

Beckmann, T., 1997: Präparation bodenkundlicher Dünnschliffe für mikromorphologische Untersuchungen. In: Stahr, K. (ed.) Mikromorphologische Methoden in der Bodenkunde. Hohenheimer Bodenkundliche Hefte 40, Hohenheim, pp 89–103.

Bell, L.S., Boydes, A., Jones, J., 1991: Diagenetic Alteration to Teeth In Situ Illustrated by Backscattered Electron Imaging, Scanning 13: 173-183

Bell L.S., 2012: Identifying post mortem microstructural change to skeletal and dental tissues using backscattered electron imaging. In: Bell, L.S. (ed.) "Forensic Microscopy for Skeletal Tissues: Methods and Protocols." MMB Series, Humana Press, Springer, New York, 173-190

Billerbeck-Braschler, S., 2016: Zug-Riedmatt - Die Tierknochenabfälle, Geweih- und Knochenartefakte aus der neolithischen Siedlung und ihre ökonomische, ökologische und kulturgeschichtliche Bedeutung. PhD thesis, University of Basel, Switzerland.

685 Billerbeck, S., Hüster-Plogmann, H., Ismail-Meyer, K., Steiner, B., Akeret, Ö., Eckmeier, E.,
686 Heitz-Weniger, A., Gross, E., Jacomet, S., Rentzel, P., Schaeren, G. and Schibler, J., 2014:
687 New taphonomic research in archaeological wetland deposits: the bone midden of Zug-
688 Riedmatt (Central Switzerland). Unpublished conference paper.

689

690 Blum, J.D., Klaue, A., Nezat, C.A., Driscoll, C.T., Johnson, C. E., Siccama, T. G., Eagar, C.,
691 Fahey, T. J. & Likens, G. E., 2002: Mycorrhizal weathering of apatite as an important calcium
692 source in base-poor forest ecosystems, Nature 417: 729-731

693

694 Blume, H.P., Brümmer, G.W., Fleige, H., Horn, R., Kandeler, E., Kögel-Knabner, I.,
695 Kretzschmar, R., Stahr, K. & Wilke B.M., 2016: Scheffer/Schachtschabel: Soil Science.
696 Springer, Heidelberg, New York, Dordrecht, London, 618 p.

697

698 Boesten, J.J.T.I., van der Linden, A.M.A., Beltam, W.H.J. & Pol, J.W., 2015: Leaching of
699 plant protection products and their transformation products; Proposals for improving the
700 assessment of leaching to groundwater in the Netherlands - Version 2. Alterra report 2630,
701 Alterra Wageningen UR (University & Research centre), Wageningen.

702

703 Brönnimann, D., Pümpin, C., Ismail-Meyer & Rentzel, P., *in press*: Excrements of omnivores
704 and carnivores. In: Nicosia, C. & Stoops, G. (eds.) Archaeological soil and sediment
705 micromorphology, Wiley-Blackwell, Chichester

706

707 Canti M.G., 2003: Aspects of the chemical and microscopic characteristics of plant ashes
708 found in archaeological soils, Catena 54: 339-361.

709

710 Canti, M. & D.J. Huisman, 2015: Scientific advances in geoarchaeology during the last
711 twenty years, Journal of Archaeological Science 56: 96 – 108

712

713 Cílová, Z., & Woitsch, J., 2012: Potash - a key raw material of glass batch for Bohemian
714 glasses from 14th -17th centuries? Journal of Archaeological Science 39: 371 – 380

715

716 Collins, M.J., Nielsen-Marsh, C.M., Hiller, J., Smith, C.I. & Roberts, J.P., Prigodich, R.V.,
717 Wess, T.J., Csapo, J., Millard, A.R.& Turner-Walker, G, 2002: The survival or organic matter
718 in bone: a review, Archaeometry 44: 383-394

719

720 Exaltus, R.P. & Miedema, R., 1994: A micromorphological study of four Neolithic sites in the
721 Dutch coastal provinces, Journal of Archaeological Science 21: 289 - 301

722

723 Fernández-Jalvo, Y, Andrews, P., Pesquero, D., Smith, C., Marín-Monfort, D., Sánchez, B.,
724 Geigl, E.-M. & Alonso, A., 2000: Early bone diagenesis in temperate environments Part I:
725 Surface features and histology, Palaeogeography, Palaeoclimatology, Palaeoecology 288: 62–
726 81

727

728 Goldberg, P & Nathan, Y., 1975: The phosphate mineralogy of et-Tabun cabe, Mount Carmel,
729 Israel, Mineralogical Magazine 40: 253 - 258

730

731 Hacket, C.J., 1981: Microscopical Focal Destruction (Tunnels) in Exhumed Human Bones,
732 Medicine, Science and the Law 21(4): 243 - 265

733

734 Hedges, R.E. M., Millard, R.A & Pike, A.W.G., 1995: Measurements and Relationships of
735 Diagenetic Alteration of Bone from Three Archaeological Sites, Journal of Archaeological
736 Science 22: 201–209

737

738 Hedges, R.E.M., 2002: Bone diagenesis: an overview of processes, Archaeometry 44: 319 -
739 328

740

741 Hoffland, E., Giesler, R., Jongmans, A.G. & Van Breemen, N., 2003: Feldspar tunnelling by
742 fungi along natural productivity gradients, Ecosystems 6: 739-746

743

744 Hollund, H.I., Jans, M. M. E. Collins, M. J., Kars, H. Joosten, I. & Kars, H., 2012: What
745 Happened Here? Bone Histology as a Tool in Decoding the Postmortem Histories of
746 Archaeological Bone from Castricum, The Netherlands, International Journal of
747 Osteoarchaeology 22: 537 – 548

748

749 Huber, R. & Schaeren, G., 2009: Zum Stand der Pfahlbauforschung in Kanton Zug. Tugium
750 25, 111-140.

Huisman, D.J., Smit, A., Jans, M.M.E., Prummel, W., Cuijpers, A.G. & Peeters, J.H.M., 2008: Het bodemmilieu op de archeologische vindplaatsen bij Swifterbant (provincie Flevoland): bedreigingen en mogelijkheden voor *in situ* behoud (Rapportage Archeologische Monumentenzorg 163), Rijksdienst voor Archeologie, Cultuurlandschap en Monumenten, Amersfoort

Huisman, D.J., (ed.), 2009, Degradation of archaeological remains, SdU Uitgevers b.v. Den Haag

Huisman, D.J. & Mauro, G., 2013: Schokland UNESCO World Heritage site 3rd monitoring round, Rapportage Archeologische Monumentenzorg (RAM) 207, Rijksdienst voor het Cultureel Erfgoed, Amersfoort

Huisman, D.J., Raemaekers, D.C.M. & Jongmans, A.G., 2009: Investigating Early Neolithic land use in Swifterbant (NL) using micromorphological techniques, Catena 78(3): 185 - 197

Huisman, D.J., Ngan-Tillard, D., Laarman, F., Tensen, M. & Raemaekers, D.C.M., 2014: A question of scales: studying Neolithic subsistence using micro CT scanning of midden deposits, Journal of Archaeological Science, 49: 585–594

Ismail-Meyer K., Rentzel P. & Wiemann P., 2013: Neolithic lake-shore settlements in Switzerland: new insights on site formation processes from micromorphology. Geoarchaeology 28: 317–339.

Ismail-Meyer, K., Vach, W. & Rentzel, Ph., *in prep.* Do still waters run deep? Formation processes of natural and anthropogenic deposits in the Neolithic wetland site Zug-Riedmatt (Switzerland).

Jans, M.M.E., Kars, H., Nielsen-Marsh, C.M., Smith, C.I.,, Nord, A.G., Arthur, P. & Earl, N., 2002: In situ preservation of archaeological bone. A histological within a multidisciplinary approach, Archaeometry 44: 343 - 352

784 Jans, M.M.E., Nielsen-Marsh, C.M., Smith, C.I., Collins, M.J. & Kars, H., 2004:
785 Characterisation of microbial attack on archaeological bone, Journal of Archaeological
786 Science 31: 87 - 95

787

788 Jans, M.M. E., 2005: Histological Characterisation of Diagenetic Alteration of Archaeological
789 Bone (published PhD-thesis). Geoarchaeological and Bioarchaeological Studies Vol. 4. Vrije
790 Universiteit Amsterdam

791

792 Jongmans, A.G., Van Breemen, N., Lundström, U. S., Van Hees, P.A.W., Finlay, R. D.,
793 Srinivasan, M., Unestam, T., Giesler, R., Melkerud, P.-A.& Olsson, M., 1997: Rock-eating
794 fungi, Nature 389: 682-683

795

796 Jorde, K., Sigmond, E.M.O. & Thorsnes, T., 1995: Stavanger, berggrunnsgeologisk kart 1:
797 250 000. Norges Geologiske Undersøkelse

798

799 Karkanas, P. & Goldberg, P., 2010: Phosphatic features, in: Stoops, G., Marcelino, V. &
800 Mees, F (eds.), Interpretation of micromorphological features of soils and regoliths, Elsevier,
801 Amsterdam, pp. 521 - 542

802

803 Karkanas, P, Bar-Yosef, O., Goldberg, P. & Weiner, S, 2000: Diagenesis in Prehistoric
804 Caves: the Use of Minerals that Form In Situ to Assess the Completeness of the
805 Archaeological Record, Journal of Archaeological Science 27: 915-929

806

807 Karkanas, P., Rigaud,J.-P., Simek, J.F., Albert, R.M., Weiner, S., 2002: Ash Bones and
808 Guano: a Study of the Minerals and Phytoliths in the Sediments of Grotte XVI, Dordogne,
809 France, Journal of Archaeological Science 29: 721-732

810

811 Keddy, P. A., 2010: Wetland Ecology: Principles and Conservation, 2nd edition. New York:
812 Cambridge University Press

813

814 Louwe Kooijmans, L.P., Van Den Broeke, P.W., Fokkens,H., & Van Gijn, A.L., 2005: The
815 Prehistory of the Netherlands, Amsterdam University Press, Amsterdam

816

Nielsen-Marsh, C.M., Hedges, R.E.M., 2000: Patterns of Diagenesis in Bone I: The Effects of Site Environments, Journal of Archaeological Science 27: 1139–1150

Nriagu, J.O. & Dell, C.I., 1974: Diagenetic formation of iron phosphates in recent lake sediments, American Mineralogist 59, 934 - 946

Out, W. A., 2010: Integrated archaeobotanical analysis: Human impact at the Dutch Neolithic wetland site the Hazendonk, Journal of Archaeological Science 37: 1521 - 1531

Polo-Diaz, A., Eguíluz, A.M., Ruiz, M., Pérez, S., Mújika, J., Albert, R.M. & Fernández Eraso, J., 2016: Management of residues and natural resources at San Cristóbal rock-shelter: Contribution to the characterisation of chalcolithic agropastoral groups in the Iberian Peninsula, Quaternary International 414, 202-225.

Pümpin, C., Wiemann, P. & Rentzel, P., 2015: Mikromorphologische Untersuchung der Schichtabfolgen. In: Bleicher, N. & Harb, C. (eds) Zürich-Parkhaus Opéra: Eine neolithische Feuchtbodenfundstelle. Befunde, Schichten und Dendroarchäologie. Vol. 1., Zürich, Egg, 152-197

Raunholm, S., Sejrup, H.P. & Larsen, E., 2003: Lateglacial landform associations at Jæren, SW Norway, and their glaci-dynamic implications, Boreas 32: 462-475

Renfrew, C & Bahn, P., 2012: Archaeology. Theory, methods, practice (6th ed.), Thames & Hudson, London

Roberts, R.J. & Brown, F.H., 1979: Authigenic mitridatite from the Shungura Formation, southwestern Ethiopia, *American Mineralogist* 64: 169 – 171

Sageidet, B. M., *in preparation*. The oldest history of the city of Stavanger, elucidated by soil micromorphology.

Sandvik, P. U., *in prep,*: Tusenårsstedet Stavanger torg: Naturvitskaplege undersøkingar. AM Oppdragsrapport 2016/06. Report to NIKU (Norwegian Institute for Cultural Heritage Research).

Shahack-Gross, R. & Ayalon, A., 2013: Stable carbon and oxygen isotopic compositions of wood ash: an experimental study with archaeological implications, Journal of Archaeological Science 40: 570-578

Shahack-Gross, R., Berna, F., Karkanas, P. & Weiner, S., 2004: Bat guano and preservation of archaeological remains in cave sites, Journal of Archaeological Science 31: 1259 - 1272

Simpson, I., Perdikaris, S., Cook, G., Campbell, J.L. & Teesdale, W.J, 2000: Cultural sediment analyses and transitions in early fishing activity at Langenesvaeret, Vesteralen, Northern Norway, Geoarchaeology 15: 743–763

Smith, C.I., Nielsen-Marsh, C.M., Jans, M.M.E. & Collins, M.J., 2007: Bone diagenesis in the European Holocene I: patterns and mechanisms, Journal of Archaeological Science 34: 1485 - 1493

Stamatakis, M. G.; Koukouzas, N. K, 2001: The occurrence of phosphate minerals in lacustrine clayey diatomite deposits, Thessaly, Central Greece, *Sedimentary Geology* 139: 33-47

Steiner, B.L., Akeret, Ö., Antolín, F., Brombacher, C., Vandorpe, P. & Jacomet, S., 2017. Layers rich in aquatic and wetland plants within complex anthropogenic stratigraphies and their contribution to disentangling taphonomic processes. Vegetation History and Archaeobotany

Stoops, G., 2003: Guidelines for analysis and description of soil and regolith thin sections, Soil Science Society of America, Madison

Stoops, G., Marcelino, V. & Mees, F. (eds.), 2010: Micromorphological features of soils and regoliths, Elsevier, Amsterdam

Tjelldén, A.K.E, Birkedal, H., Lomholt, S & Rejnmark, L., *in press,* Advantages and limitations of HR-pQCT scans in documenting archaeological human bone diagenesis, Archaeometry

Tjelldén, A.K.E., 2016: Death, dacay and dissolution? The impact of wetland environment on archaeological bone, PhD thesis Aarhus University, 158 pp.

Trueman, C.N.G. & Martill, D.M., 2002: The long-term survival of bone: the role of bioerosion, Archaeometry 44: 371-382

Turner-Walker, G., 2009: Degradation pathways and conservation strategies for ancient bone from wet anoxic sites, In: Straetkvern, K. & Huisman, D.J., Proceedings of the 10th ICOM Group on Wet Organic Archaeological Materials Conference, Amsterdam 2007, Nederlandse Archaeologische Rapporten 37, Rijksdienst voor Archeologie, Cultuurlandschap en Monumenten, Amersfoort, pp. 659 - 676

Turner-Walker, G., 2012: Early bioerosion in skeletal tissue: persistence through deep time., Neues Jahrbuch für Geologie und Paläontologie, Abhandlungen 256(2): 165 – 183

Turner-Walker, G. & Jans, M.M.E., 2008: Reconstructing taphonomic histories using histological analysis., Palaeogeography, Palaeoclimatology, Palaeoecology 266: 227 – 235

Villagran, X, D.J. Huisman, C. Miller, S. Mentzer & M.M.E. Jans *in press*, Bone and other skelettal tissues, In: Nicosia, C. & Stoops, G. (eds.) Archaeological soil and sediment micromorphology, Wiley-Blackwell, Chichester

Wallander, H., 2000: Uptake of P from apatite by Pinus sylvestris seedlings colonised by different ectomycorrhizal fungi, Plant and Soil, 218: 249-256

Wood, W.R. & D.L. Johnson, 1978: A survey of disturbance processes in archaeological site formation, Advances in Archaeological Method and Theory 1: 315 - 381

913

914 www.mindat.org, last accessed 29-6-2016

List of figures

Figure 1 Polished sections of the profile column ZGRI 84 (upper part left side, lower part in the middle) and ZGRI 98. The sections go through the grey, natural, limnic carbonates at the base (sections ZGRI 84B 0-4 cm and 98 0-3 cm) and the bone midden (ZGRI 98 3-18 cm, ZGRI 84B 4-23 and ZGRI 84A 0-24 cm) rich in dark organic layers and heterogeneous, grey loam- and ash-rich deposits. The position of the taken thin sections is marked in blue. Beside the polished sections are scans of the corresponding thin sections, with the position of micrographs marked in black (see Figure 4). Note the large bones (b) in the polished section 84A, and the fish bone and ash accumulation in the middle part of the section 98 (see also Figure 4K, L). The SEM and EDX measurements have been made on section 84A (see Figure 9).

Figure 2 Hazendonk thin section 77110 (see Exaltus and Miedema 1994 for the profile). A: Scan of the thin section, containing a layered peat deposit with sandy peat domains (s). Fissures were formed during the preparation of the thin section. B: Enlargement of part of A with bone layers. C: Same as B, indicating bone layers (grey) and charcoal (black)

Figure 3 Stavanger Mi-5 thin section. A: Scan of the thin section. Note charcoal fragments (one indicated with “c”) and rockfragments (“r”). B: Drawing of the thin section, indicating the fragments of strongly decayed bone and the area of image C. C: Low-magnification micrograph of decayed-bone area. The bone remain is visible as an orange groundmass.

Figure 4 Bone decay features in the Zug-Riedmatt sample. All images in plane polarized light (PPL) unless indicated otherwise. A: Bone or antler fragment with cyanobacterial tunnelling from the surface to a depth of c. 50 micron from the bone surface. B: Same as A with crossed polarizers (XPL) showing the good preservation of the bone microstructure. C: Same as A under fluorescent light. The highly fluorescent objects in the top of the image are a flaxseed and a wood fragment. D: Bone or antler fragment, showing excellent preservation in general, but some darker regions where chemical/mineralogical changes have occurred. E: Enlargement of part of D, showing the darker colour and shrinkage cracks in some of the affected regions. F: Same as E under fluorescent light showing a loss of fluorescence in the affected regions. G: Spongeous bone with at the surface dissolution and cracking features. H: Enlargement of a part beside G. I: Same as H with crossed polarizers (XPL) showing the clear birefringence in the well preserved left part and the complete loss of birefringence in the affected part of the bone. J: Same as H under fluorescent light showing the loss of

fluorescence in the affected part. K: Accumulation of fish scales and/or gills (all bone in the image; typical saw-tooth edges indicated with (s) and (greyish) calcitic ashes (a), showing spherical (newly formed) shapes (arrow). L: Same as K under fluorescent light. The scales show parts with loss of fluorescence, similar to J, close to the ashy region. Fluorescence is retained in the rest of the scales; the newly formed object has a higher fluorescent intensity (arrow), as well a thin layer on some of the scales. M: Animal bone or antler with tunnelling (arrow) and darker parts. N: Same as M under fluorescent light showing fluorescence in the tunnelled zones and a loss of fluorescence in the darkened parts.

Figure 5 Bone decay features in the Hazendonk sample. All images in plane polarized light (PPL) unless indicated otherwise. A: Fish scales showing extensive tunnelling. B: Fish scale with extensive decay inside, leaving only the outer rim unaffected. Note breakage at the left of the fish scale. C, D: Massive orange-yellow material with bone fragments and fish scales, intercalated between peat and ashes with charcoal. D in XPL, note lack of birefringence of the massive material and birefringent bone fragment in the right of this layer. E, F, G: Massive material and bone fragments. F with blue light fluorescence, G with UV fluorescence. The red circle in the three micrographs surrounds an area of fine spongeous bone that is visible in UV fluorescence (G), but not in PPL or Blue light fluorescence (E,F). H, I: Massive orange-yellow material with deformation features due to intrusive fragment of burnt bone (centre top), and showing extensive tunnelling. I with incident light.

Figure 6 Bone decay features in the Stavanger sample. A, D in PPL; B, E in XPL, C, F in Blue light fluorescence. A, B, C: Bone, strongly broken up into angular blocky fragments. Orange-yellow material precipitated in the fissures. Black stains due to precipitation of manganese compounds. The bone fragments are isotropic, as is the orange-yellow like material. Both are slightly fluorescent. D, E, F: Strongly fragmented bone with orange-yellow material, which here also contains fan-shaped precipitates. Some areas show increased fluorescence.

Figure 7 SEM-results for the Zug-Riedmatt sample ZGRI 84A. A: Backscatter image with well-preserved bone, showing a smooth surface. B: Idem, with decayed bone showing a pattern of fissures. C: EDX spectrum of spot analyses in figure A. D: EDX spectrum of spot analyses in figure B.

Figure 8 SEM-results for the Stavanger sample. A: Backscatter image with well-preserved (smooth surface) and decayed (grainy) bone. Spot analyses are marked, and the spectra are given in B and C. D-G: SEM-EDX mappings for mappings for Ca (D), P (E) and Fe (F). Note the lower Ca and higher Fe in the grainy material.

Figure 9 Comparison of the EDX analyses of bone in the Zug-Riedmatt and the Stavanger samples. The ideal (stoichiometric) composition of common Ca- and Ca, Fe-phosphate minerals have been plotted as well for comparison. A: Relation between Ca and PO_4 (recalculated from P). The Zug-Riedmatt samples all have the same Ca/PO_4 ratio, but the degraded parts have lower concentrations. The Stavanger samples, however, including the seemingly well-preserved bone, have lower Ca/PO_4 ratios. B: Relation between Ca/PO_4 and Fe/PO_4. All Zug-Riedmatt samples fall in a tight cluster close to hydroxyapatite. The degraded Stavanger samples fall close to mitridatite. The other Stavanger measurements lie between hydroxyapatite on the one hand and the group of anapaite, calcioferrite and mitridatite.

List of tables

Table 1 General Histological Index (GHI): after Hollund et al. (2012) with minor modifications.

GHI	Approximate % of intact bone	Description
0	0-5	No original features identifiable, except maybe Haversian channels
1	5-15	Small areas of well-preserved bone present, or the lamellate structure is preserved by the pattern of destructive foci
2	15-50	Some well-preserved bone present between destroyed areas
3	50-85	Larger areas of well-preserved bone present
4	85-95	Bone is fairly well preserved with minor amounts of destroyed areas
5	95-100	Very well preserved, similar to modern bone

Table 2 Overview of sites and the samples used in this study.

Site	Age (cal.)	Landscape setting	Type of site	Type of archeological deposit	Basal sediment	Soil sample	Thin section size (cm)
Zug-Riedmatt	3200 - 3100 BC	pre-Alpine lake shore	Lake dwelling	Bone midden	Lake marl (micrite)	ZGRI 84A/B, 98A	4,5 x 4,5
Hazendonk	4000 BC	River delta	River dune flank	Refuse deposit	Sand, peat, clay	77110	8 x 16
Stavanger	900 - 1100 AD	Coastal	Historic market place	Ancient shore line	Gravel from gneisses	5	8 x 5

1014 Table 3 Analytical results of the SEM-EDX analyses. "Altered bone" is visibily altered on a
1015 microscale in the SEM-BSE images; see the BSE images in Figure 7 and 8.

1016

Measurement	Altered (A) or unaltered (U) bone	PO_4 (%)	Ca (%)	Fe (%)
Stavanger 2 - 1	A	33.3	7.9	16.2
Stavanger 2 - 2	U	41.3	20.4	7.7
Stavanger 7 - 1	A	37.2	7.8	20.5
Stavanger 7 - 2	U	40.9	19.4	8.2
Stavanger 7 - 3	U	34.9	14.5	11.1
Stavanger 9 - 1	A	38.3	10.3	18.7
Stavanger 9 - 2	A	39.3	9.6	20.6
Stavanger 9 - 3	A	29.6	8.6	16.8
Zug - Riedmatt 1 - 1	U	53.9	39.5	3.4
Zug - Riedmatt 3 - 1	U	47.2	35.3	3.4
Zug - Riedmatt 4 - 1	A	43.9	34.3	2.9
Zug - Riedmatt 6 - 1	A	46.6	33.7	2.7
Zug - Riedmatt 7 - 1	A	35.5	27.2	2.7
Zug - Riedmatt 8 - 3	U	48.5	37.5	3.1
Zug - Riedmatt 9 - 2	A	46.7	36.3	1.9
Zug - Riedmatt 11 - 1	A	43.0	34.1	3.1
Zug - Riedmatt 11 - 2	A	41.8	31.1	2.6
Zug - Riedmatt 12 - 2	A	45.5	34.9	2.8
Zug - Riedmatt 13 - 1	A	37.7	29.3	2.7

1017

1018

1019

1020 Table 4 Summary of observed bone decay features

1021

Site	Soil sample	GHI	Mfd sites	Tunneling	Darkening and micro-aggregation	Dissolution + cracking/ fragmenting	Ca, Fe phosphate precipitates
Zug-Riedmatt	ZGRI 84a	4-5				Localized, surfaces only	
	ZGRI 84b	4-5		Cyanobacterial surface tunnelling in some bones			
	ZGRI 98	4-5		Cyanobacterial surface tunnelling in some bones	Localized (fish scales)		
Hazendonk	77110	0-1	Complete (fish scales)	Complete Wedl tunneling in fish scales			Forming a layer with embedded bone fragments
Stavanger	5	0				Complete	Inside the bone fragments

1022

Figure 1

Click here to download high resolution image

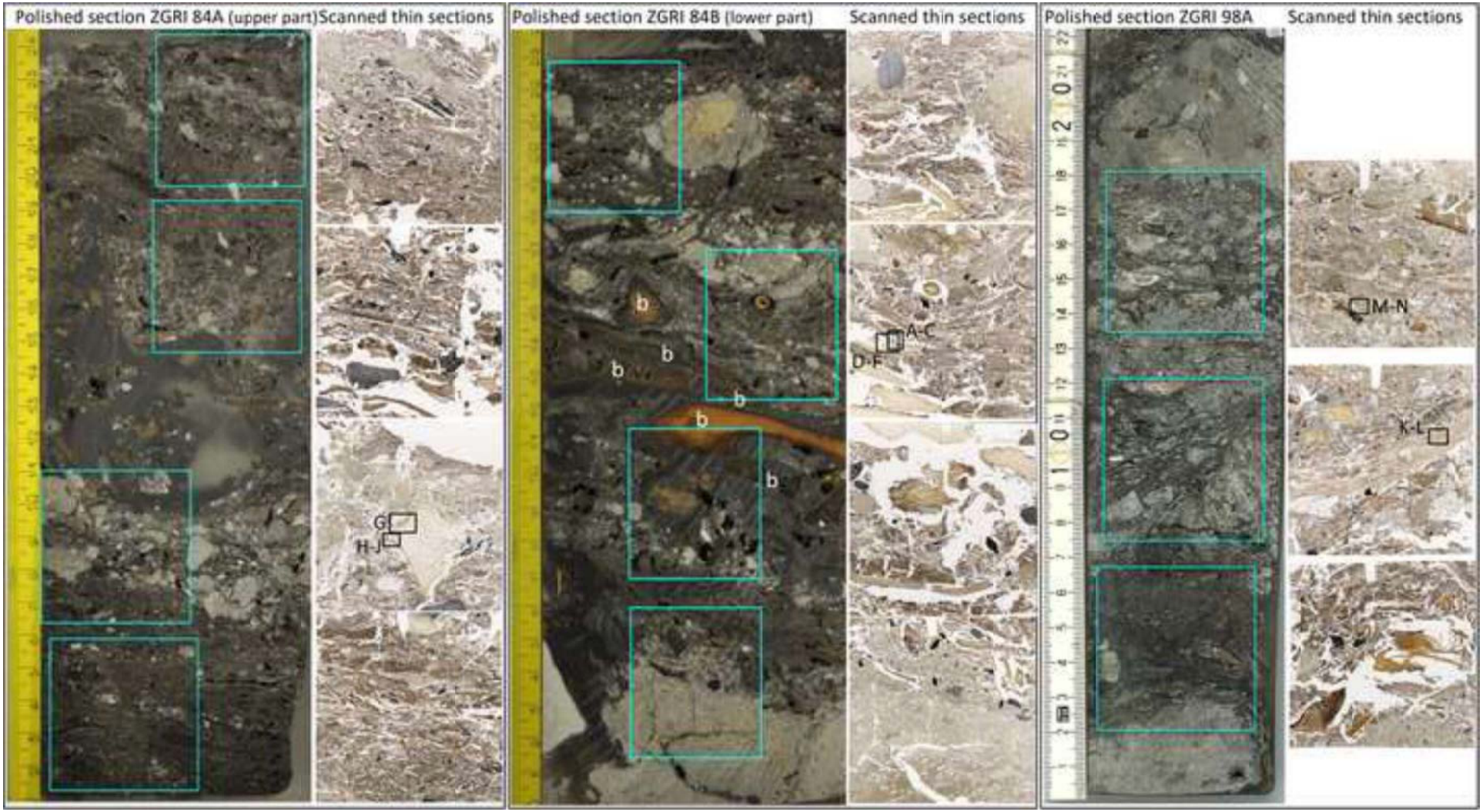

Figure 2

Click here to download high resolution image

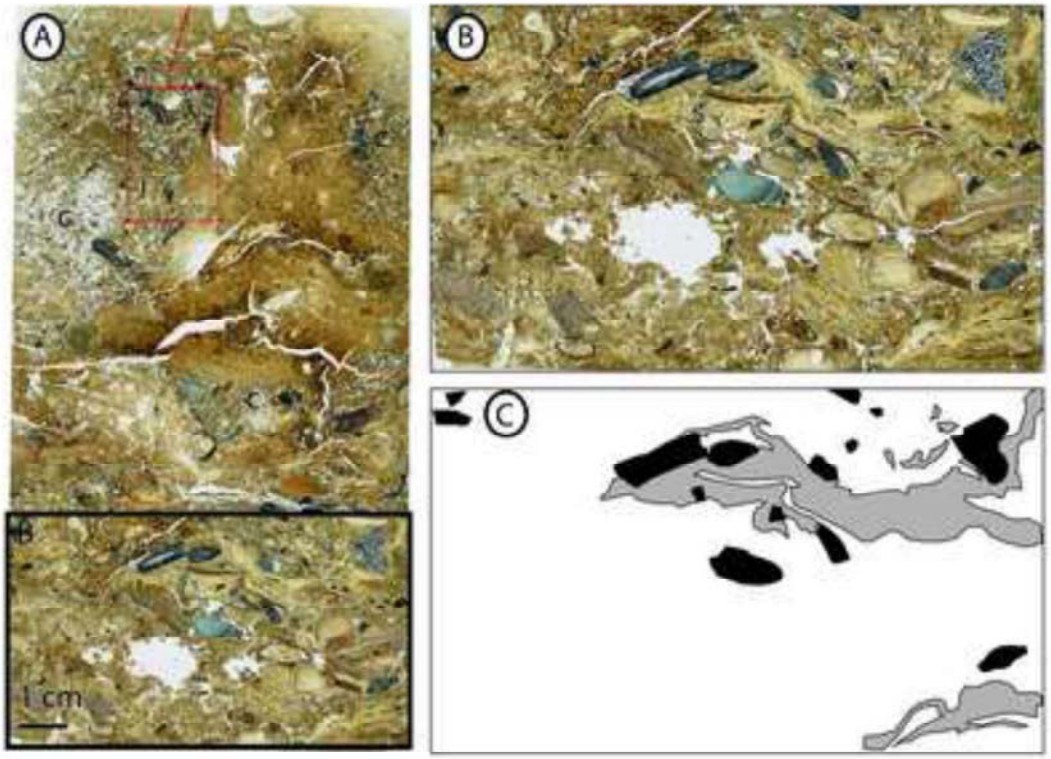

Figure 3

Click here to download high resolution image

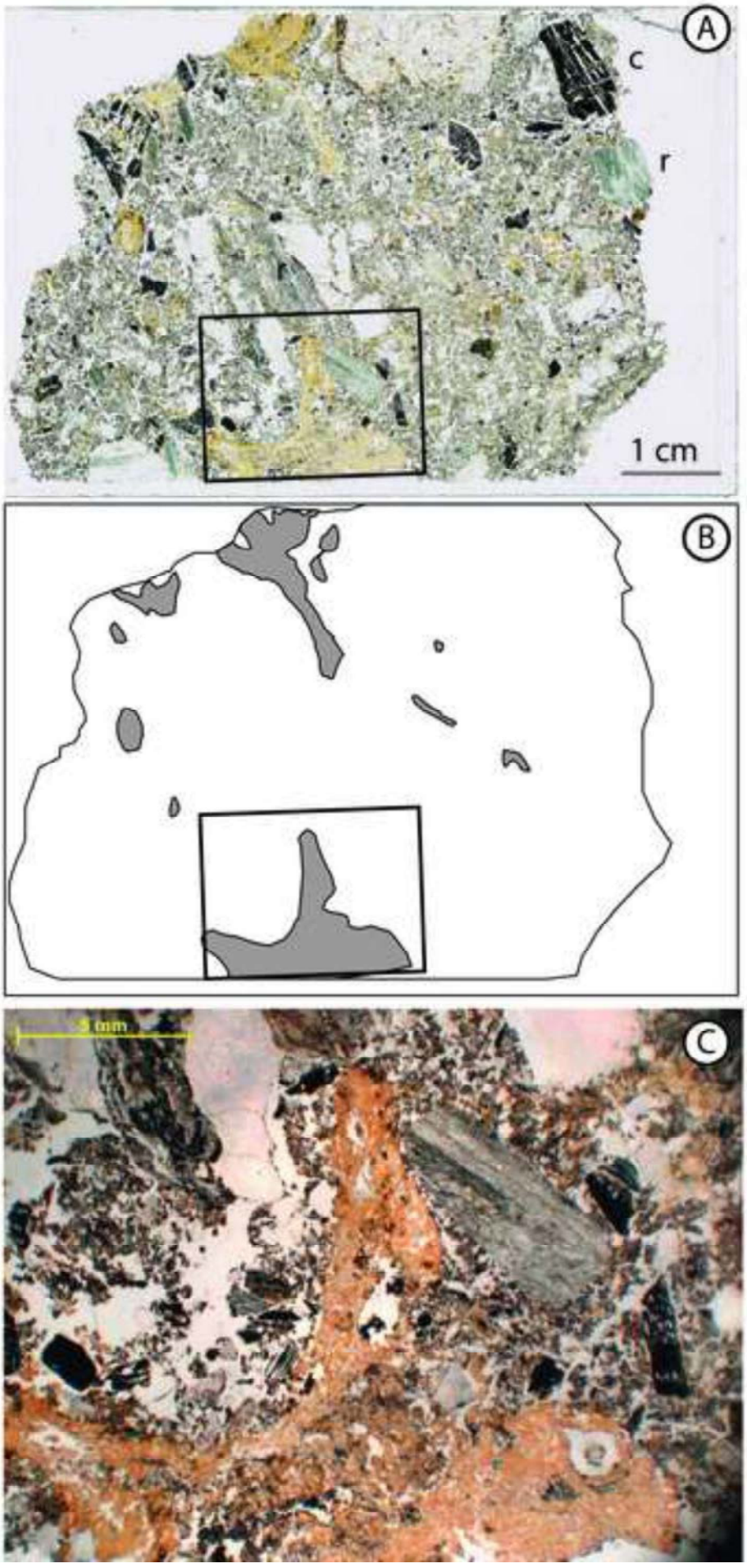

Figure 4 A-F

Click here to download high resolution image

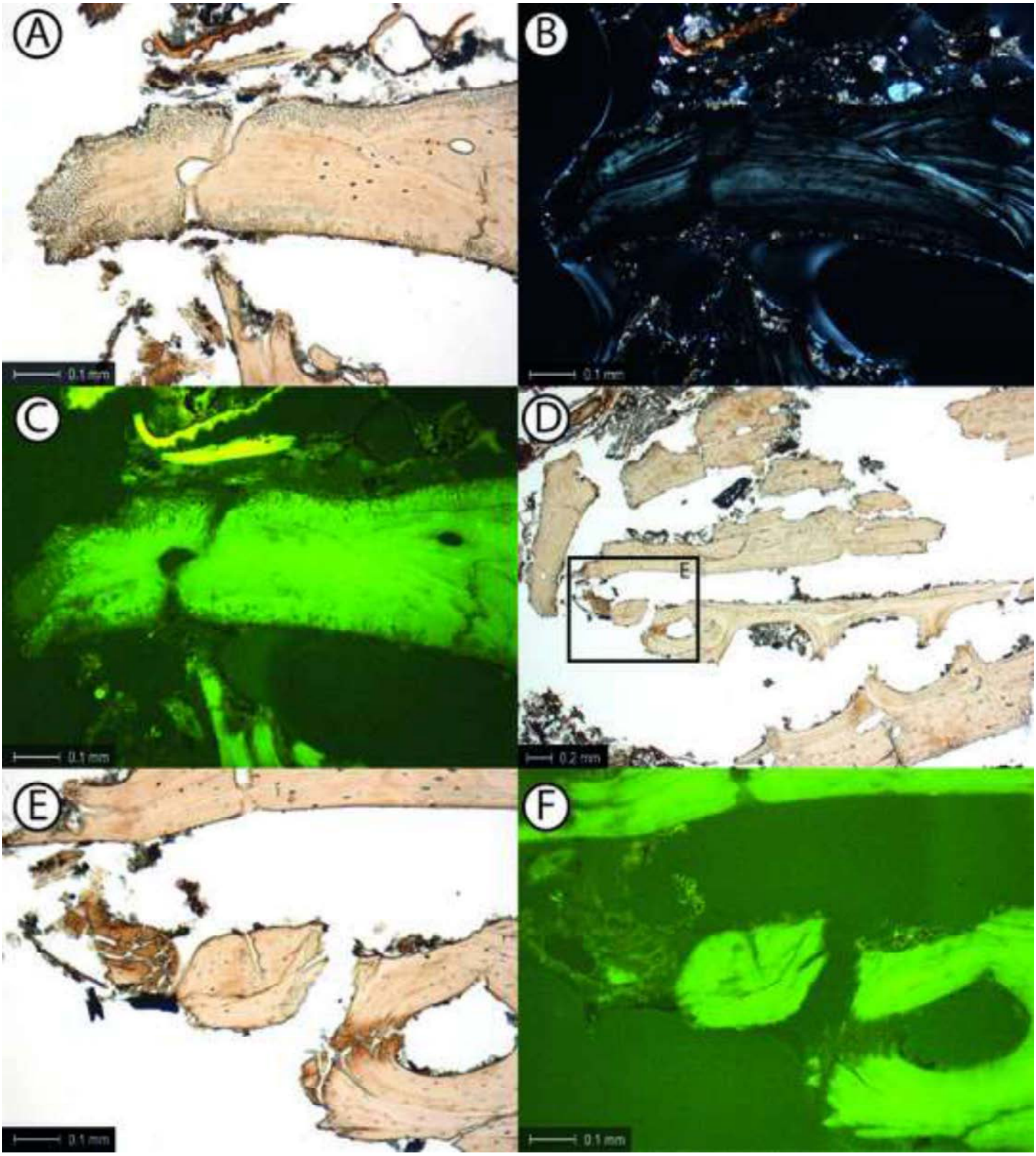

Figure 4 G-O

Click here to download high resolution image

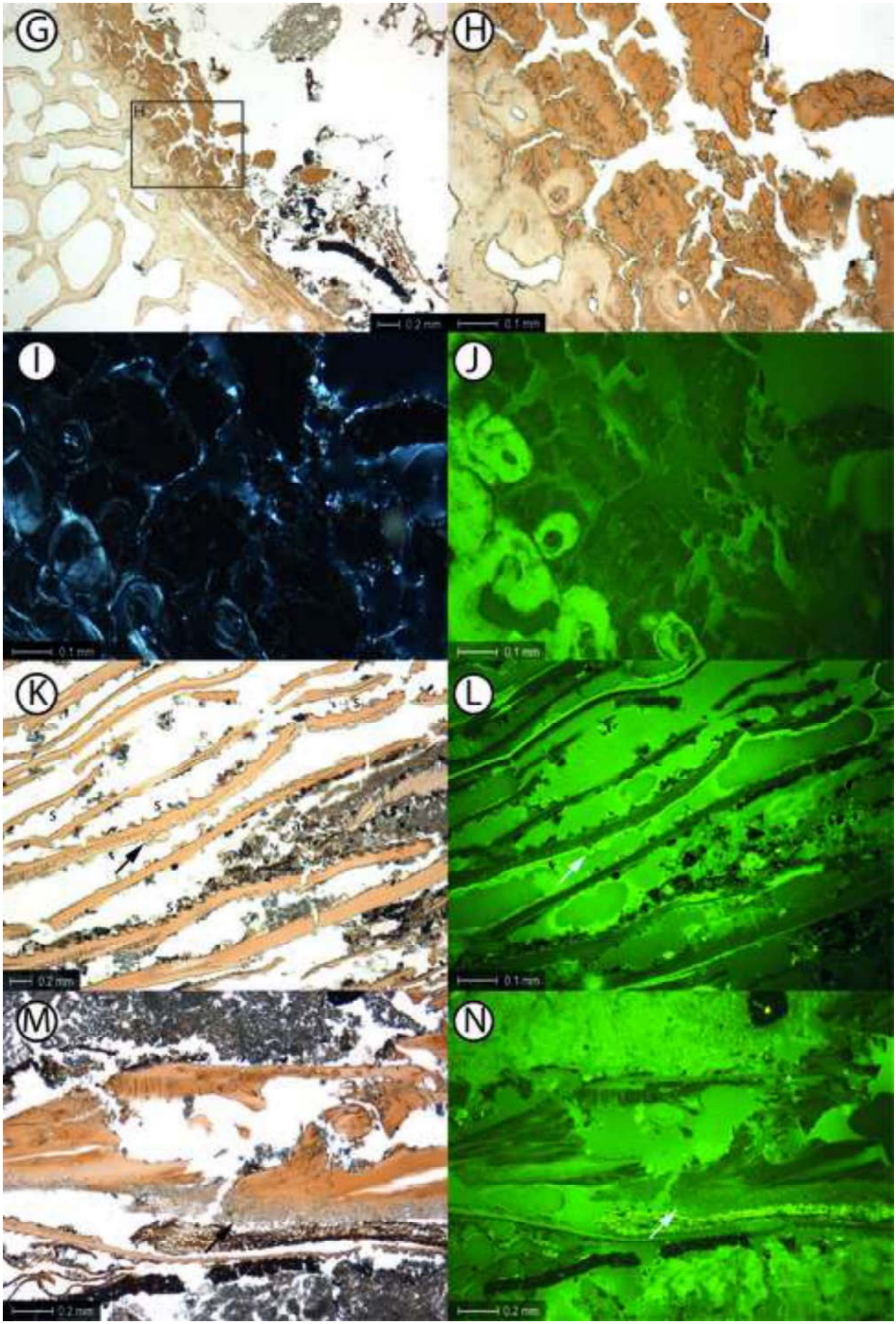

Figure 5 A-D

Click here to download high resolution image

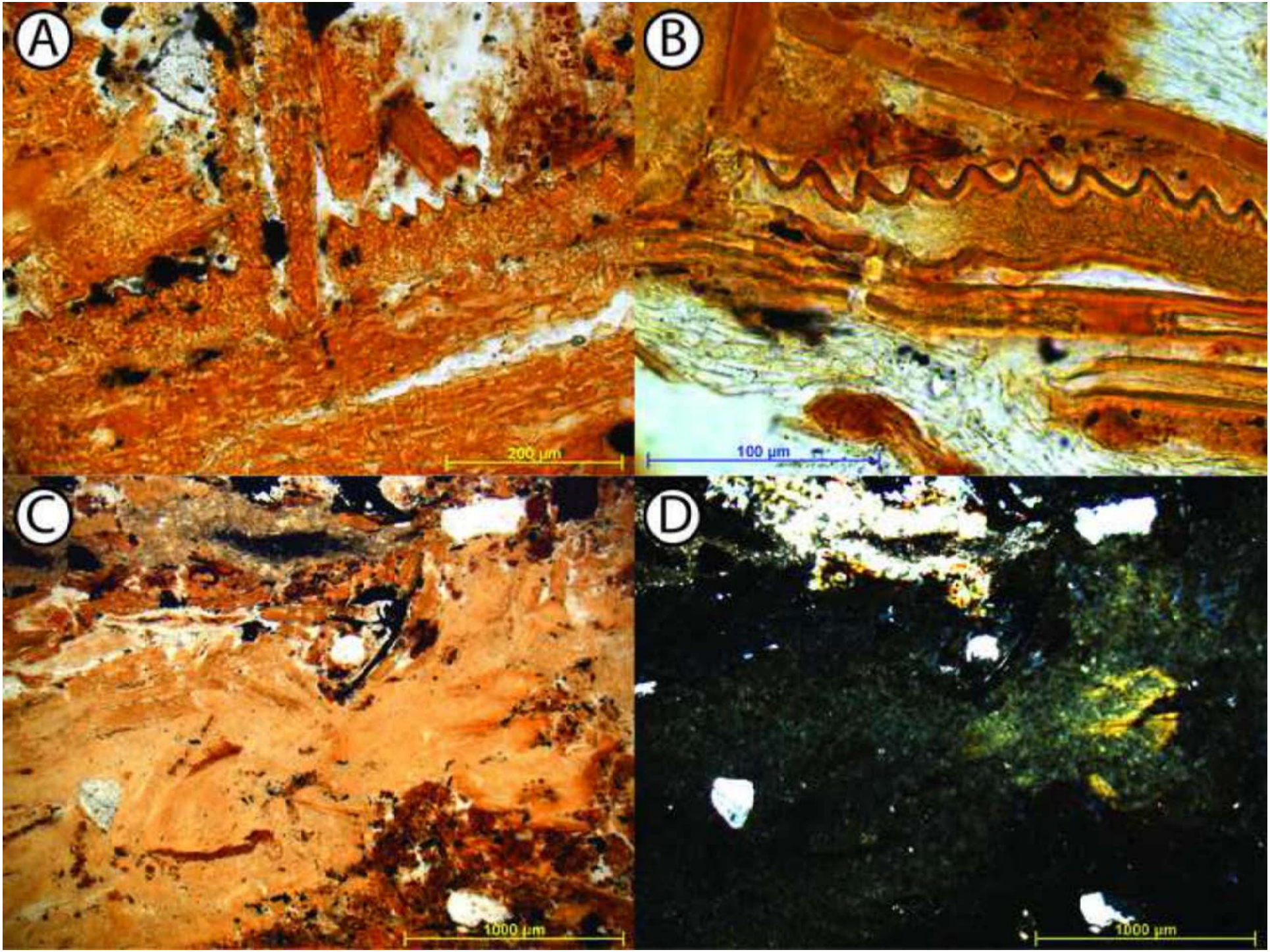

Figure 5 E-I

Click here to download high resolution image

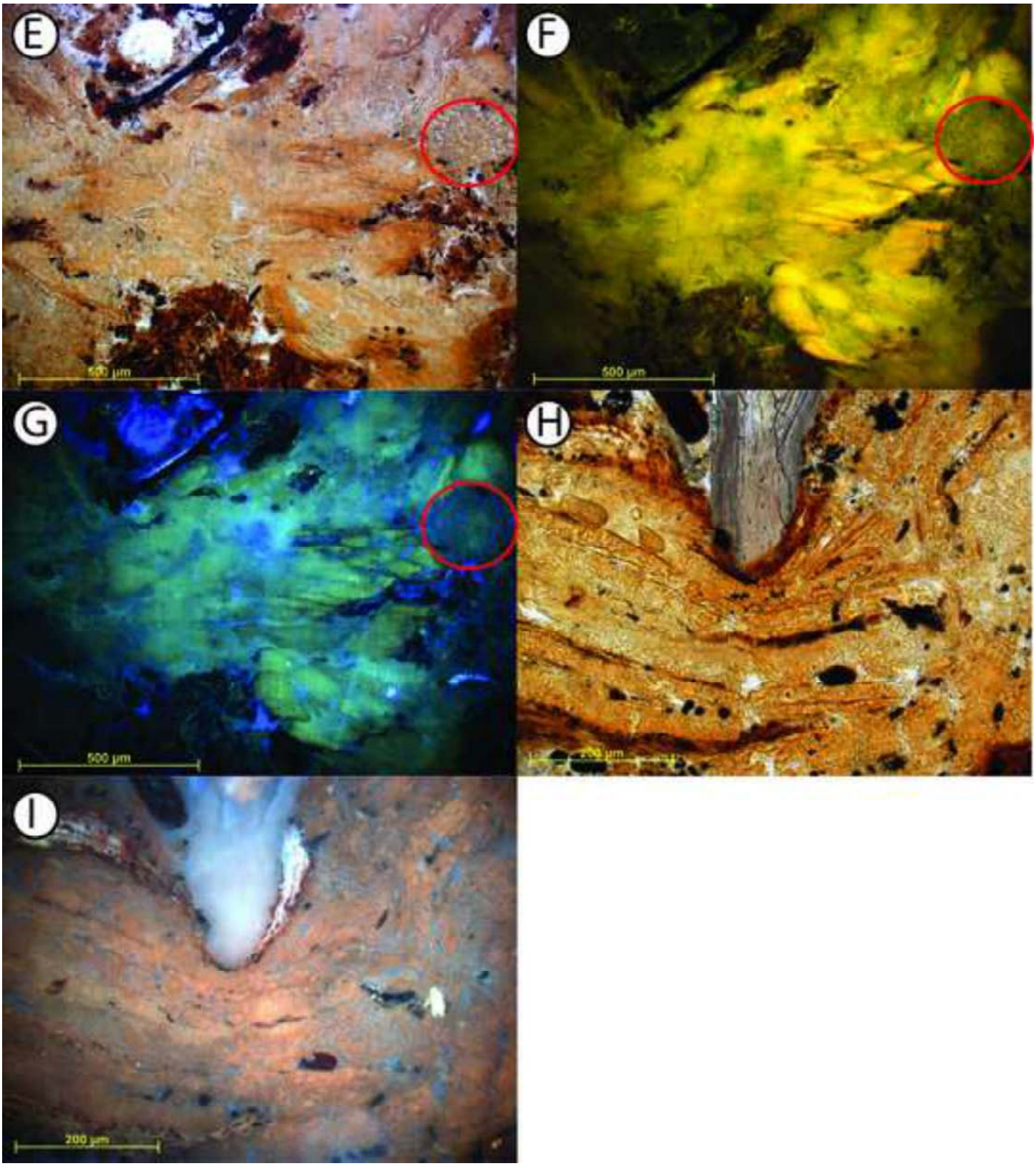

Figure 6

Click here to download high resolution image

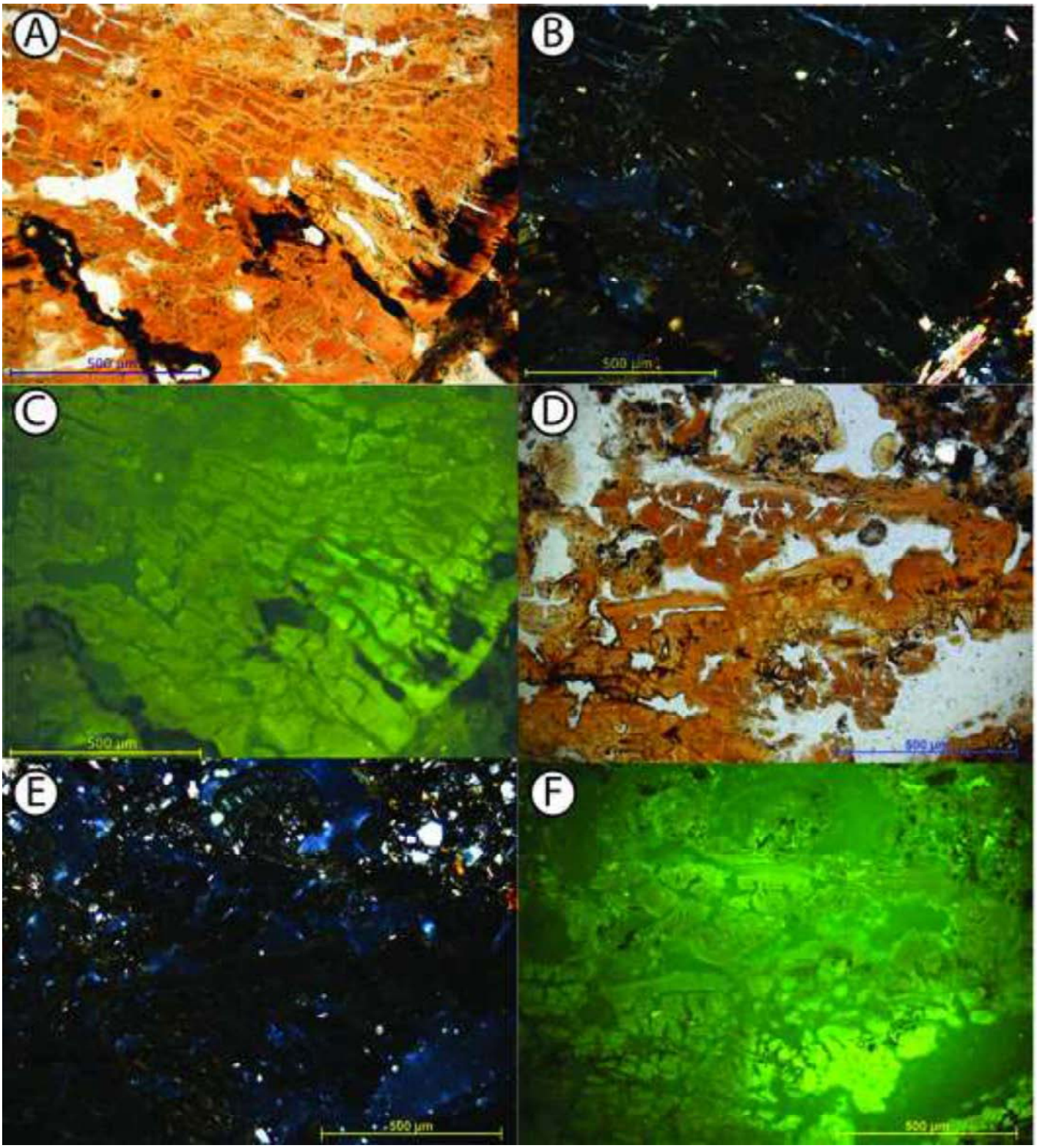

Figure 7

Click here to download high resolution image

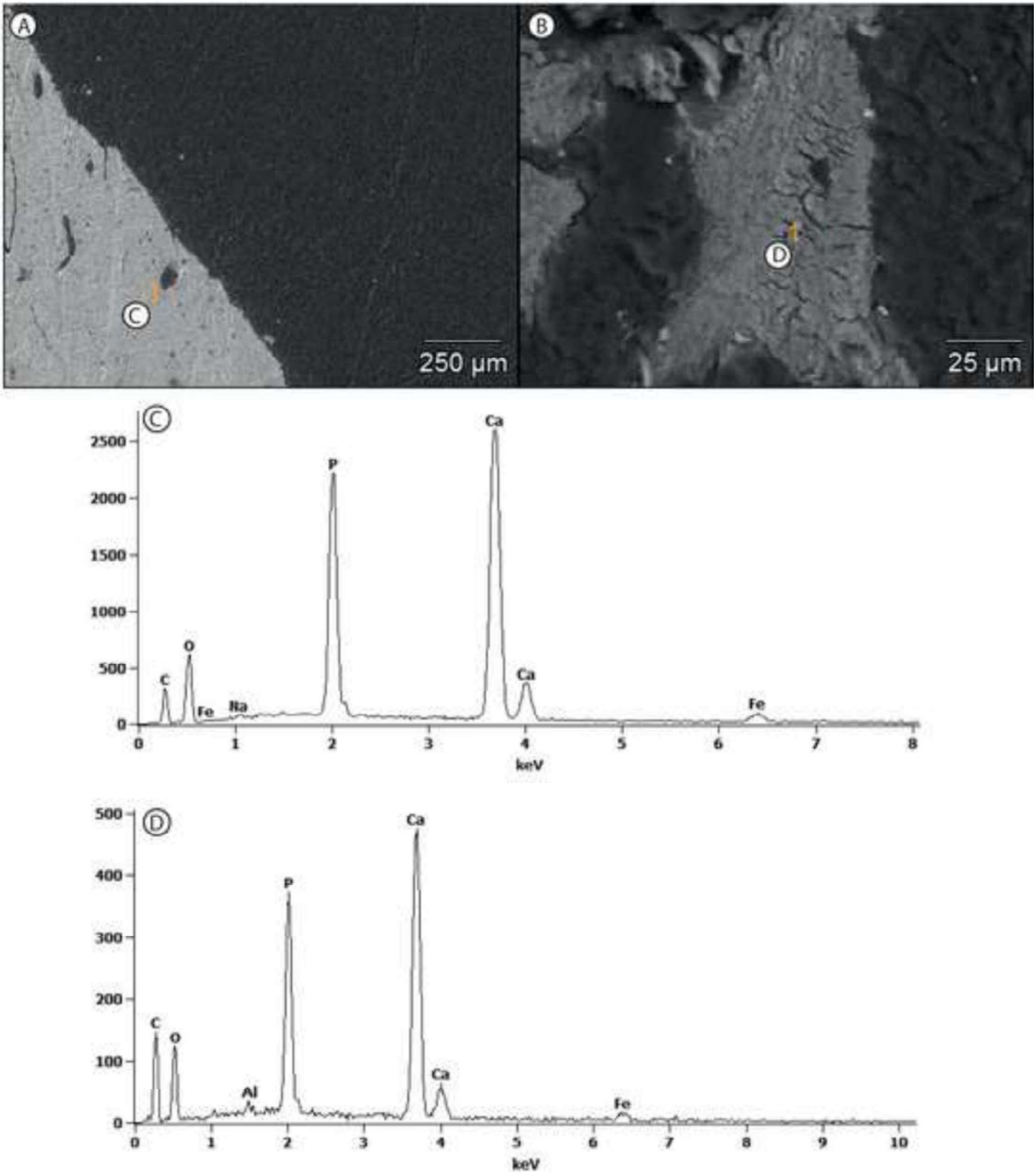

Figure 8

Click here to download high resolution image

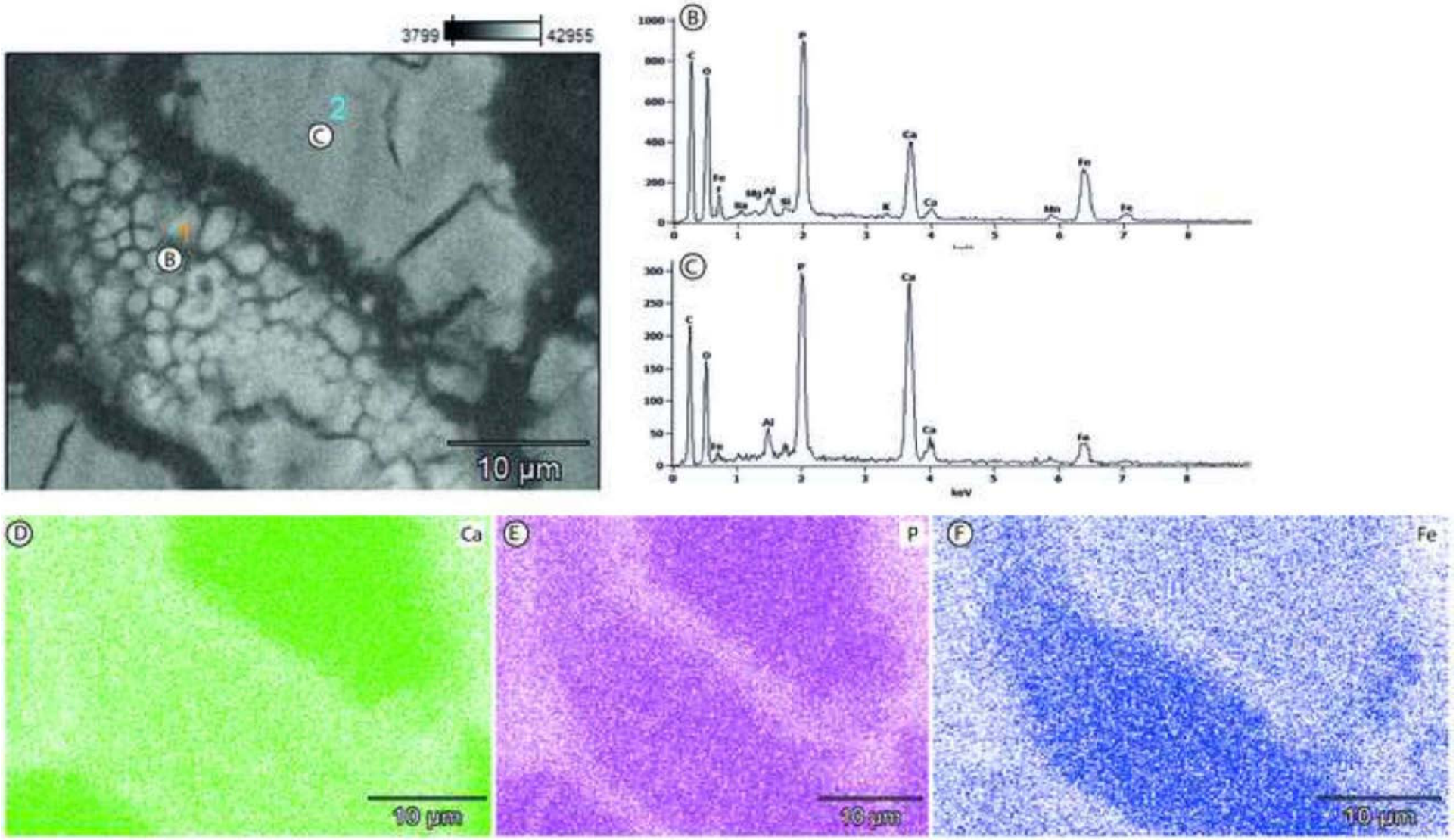

Figure 9A
Click here to download high resolution image

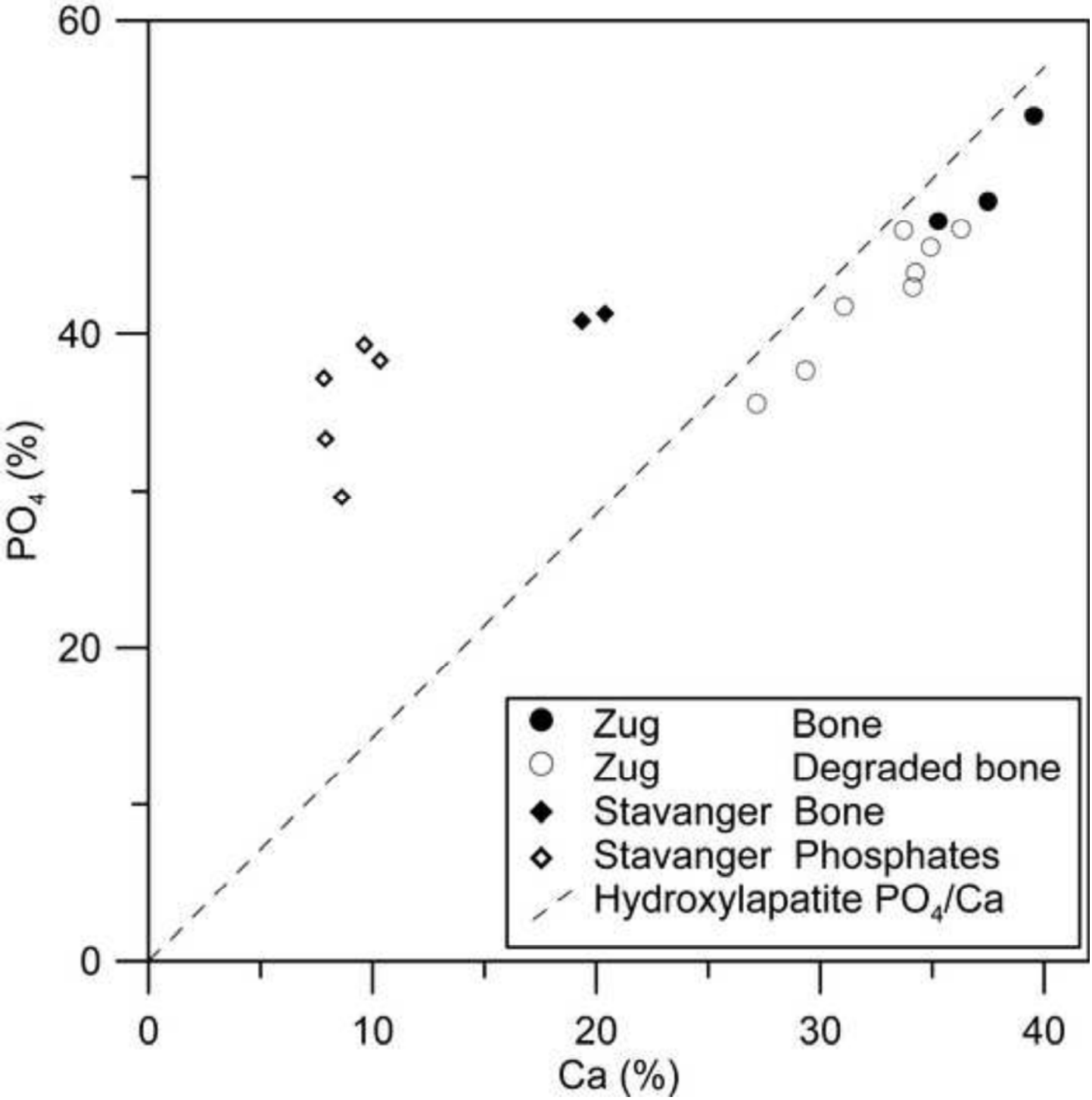

Figure 9B

Click here to download high resolution image